Chapter 4

Automated matching of lung nodules on follow-up CT scans

Automated matching of lung nodules is another important function required for a chest CAD system. This chapter introduces a novel method for automated matching of lung nodules that are segmented from follow-up chest CT images by the method introduced in chapter 3. The proposed nodule matching method is based on rigid and non-rigid registration techniques and a similarity calculation procedure. The similarity calculation procedure includes three patterns for similarity measurements based on the consideration of nodules with temporal changes in follow-up CT images.

4.1 Purpose

The observation of small pulmonary nodules on follow-up CT images is an important approach for the malignancy diagnosis of SPN and the effective analysis of treatment. However, the observation of nodules on follow-up CT images takes greatly burdens on physicians. This is because thin-section CT images often have a large number (typically 300-500) slice images of 1mm section, and the lesions usually attach to anatomic structures such as vessels, the heart and diaphragm. Especially, in the case of metastatic lung cancer, hundreds of nodules may exist in follow-up CT images. Furthermore, the different poses of a patient on the CT table and the effects of heartbeats and respiratory

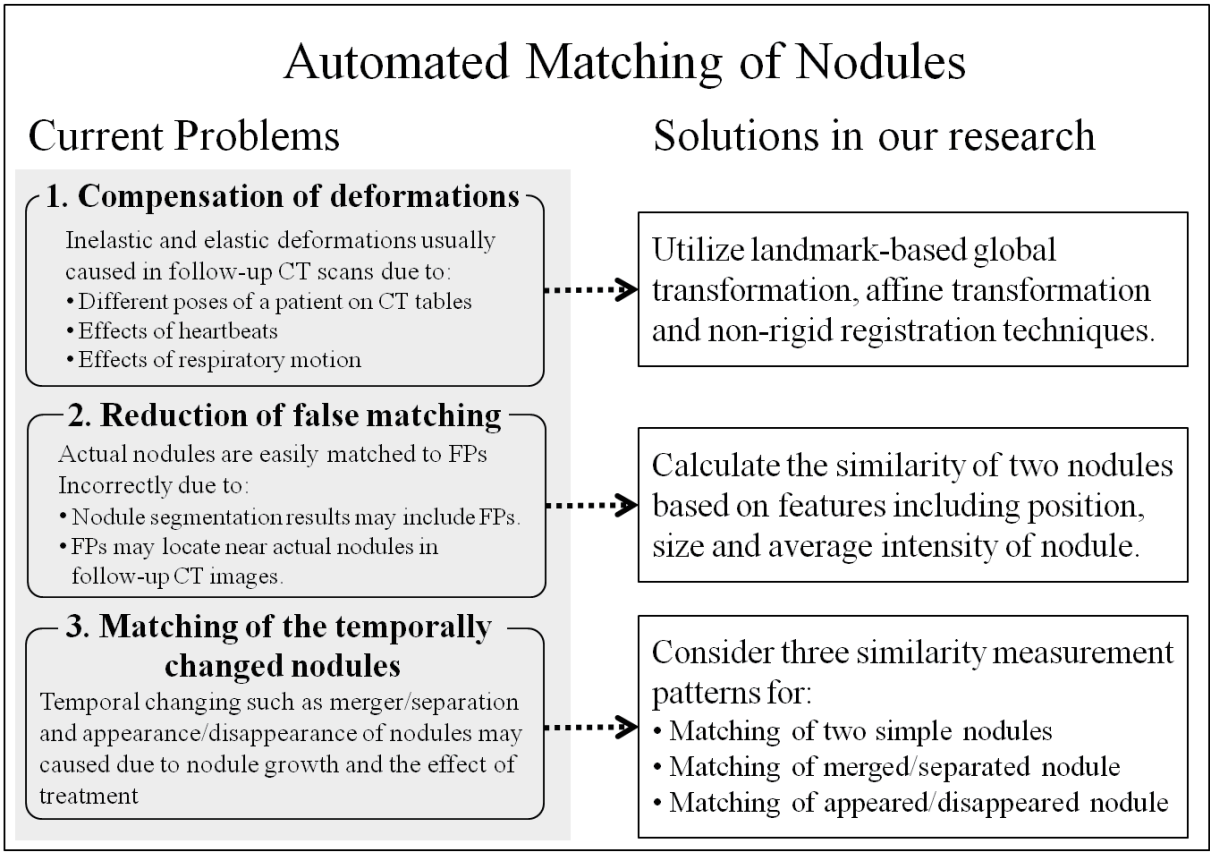

Figure 4.1: The problems in the nodule matching and the solutions of the proposed method

motion usually cause both inelastic and elastic deformations in follow-up CT images. To lighten such burdens, the development of automated nodule matching methods for assisting the observation of nodules on follow-up CT images is required.

However, to find the corresponding nodules in follow-up CT images suffers the following problems (Fig. 4.1):

(1) Inelastic and elastic deformations are usually caused due to the different poses of a patient on the CT tables, the effects of heartbeats, and respiratory motion. Such deformations have to be compensated for the corresponding nodule finding.

(2) It is difficult to avoid the false matching of actual nodules and FPs, when the automatic nodule segmentation results include many FPs.

(3) Due to the growth of nodules and the effects of treatment, the merger (two separated nodules in a past CT image merge to be one nodule in current CT image), separation (one nodule in a past CT image separates to be two nodules in current CT image), and appearance (a new nodule generated in current CT image), disappearance (a nodule in a CT image disappears in current CT image) of nodules may occur. To match such temporal changed nodules is challenge.

To deal with the above problems, we will introduce the following three solutions (Fig. 4.1):

(1) Utilization of a landmark-based global transformation, the affine registration and the non-rigid registration scheme to co-register follow-up CT scans for compensating lung deformations.

(2) Calculations of the similarities between two nodules based on feature vectors including the information of position, size, and average intensity of each nodule. The previous method [158] only used the nodule position to calculate the similarities; however, if an FP in the past (current) CT images is located near an actual nodule in current (past) CT images, the false matching could easily occur when only considering their positions. The proposed method utilizes the information of nodule size and average intensity to restrict the similarity calculation.

(3) Consideration of three patterns for similarity calculation, which correspond to the matching of nodules without temporal changes (normal nodules), merged/separated nodules, and appeared/disappeared nodules, respectively.

4.2 Methods

4.2.1 Overview

Figure 4.2 shows a flowchart for the proposed method. The proposed method consists of four main procedures : (a) preprocessing, (b) registration of follow-up CT images,

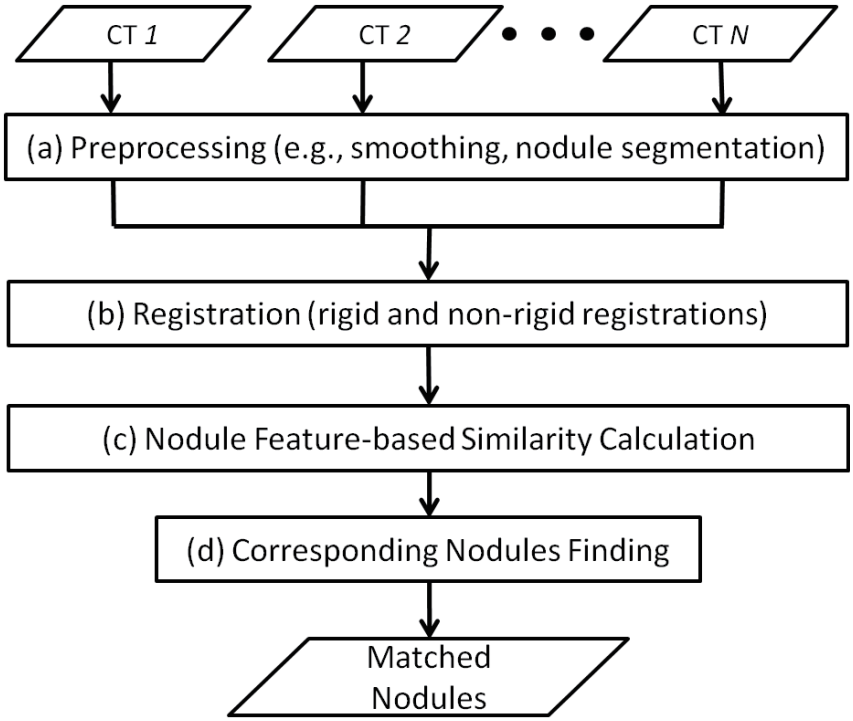

Figure 4.2: Flowchart of the proposed methods.

(c) similarity calculation and (d) corresponding nodules finding from every two registered CT images. In step (a), a smoothing process and the extraction of lung regions is performed for each input chest CT image. Then, the nodule candidates are segmented by the automated nodule segmentation method introduced in Chapter 3 in this dissertation. In Step (b), the initial scan is considered the reference scan, and all follow-up CT images are registered to it. The registration procedure includes two rigid registrations a the non-rigid registration. Finally in Step (c), we find corresponding nodules from every two registered CT images by calculating the similarity of nodules. We define the same nodules that are matched in all the CT images of one patient as "same nodule group", and the nodules belonging to a "same nodule group" is marked by the same ID.

4.2.2 Preprocessing

For each input 3D chest CT image, a preprocessing procedure is performed first. Four processes are implemented in turns as following:

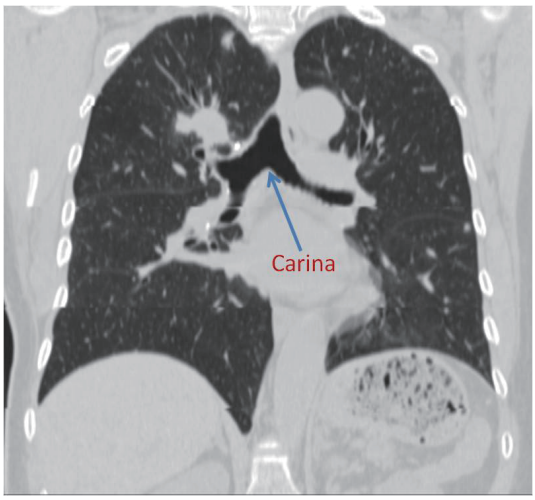

(a) Carina

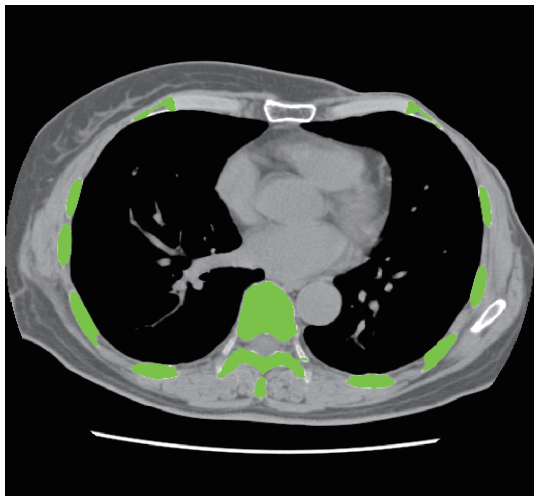

(b) Ribs

Figure 4.3: Landmark segmentation. (a) Carina point, and (b) Rib bones (marking in green)

(1) Smoothing: A median filter whose mask size is $3 \times 3 \times 3$ voxel is utilized to remove the image noise.

(2) Extraction of lung area: The lung region extraction method introduced by Kitasaka et al. [141] is utilized to extract lungs area R_{lung} from each CT image.

(3) Segmentation of lung nodules: Our automatic lung nodule segmentation method introduced in Chapter 3 is applied to segment the nodules from each lungs area R_{lung}.

(4) Segmentation of carina and ribs: We detect the carina point and ribs region as the landmarks of registration process from each input CT image (Fig. 4.3). The carina is detected by the method reported in [140]. The ribs are extracted by a single thresholding procedure.

4.2.3 Registration of CT images

The different poses of a patient on the CT table, the effects of heartbeats, and the respiratory motion usually cause the inelastic and elastic deformations in follow-up CT images. To find the corresponding nodules, the registration of all follow-up CT images

of a patient is required. We consider the first scan as a reference image, so that all the later scans (registered scan) are co-registered to the first scan. However, the registration procedure is only applied inside the lung regions R_{lung}. Our registration consists of three steps:

(1) A global landmark-based transformation is performed to roughly compensate the deformation. The carina point detected from each input CT image is utilized as a landmark (Fig. 4.3(a)). Each registered scan is transformed to match the reference scan by the positions of their carina points.

(2) An affine registration is performed to compensate for global motion such as rotation, translation, scaling and shearing of the lung. The extracted rib regions (Fig. 4.3(b)) are utilized as landmarks for transformation, since the ribs generally move together with the lungs during respiration or heartbeats.

(3) An improved non-rigid registration model [162] using a discrete Markov Random Field objective function is applied to compensate for the elastic deformation of lung area due to respiration and heartbeats of the patient.

By performing these registration processes, anatomical objects inside the lung areas such as blood vessels and lung nodules in different CT images are accurately aligned for further analysis.

4.2.4 Similarity calculation of nodules

4.2.4.1 Similarity measure

The corresponding nodules are found from all of the automatically segmented nodules of every two follow-up CT images. Figure 4.4 shows an example of nodule matching of two CT images (I_a and I_b). The corresponding nodules are found via a similarity measure based on features that include the coordinates of centroid ($\mathbf{g}$), diameter ($\mathbf{d}$), and average intensity ($\mathbf{I}$) of a nodule.

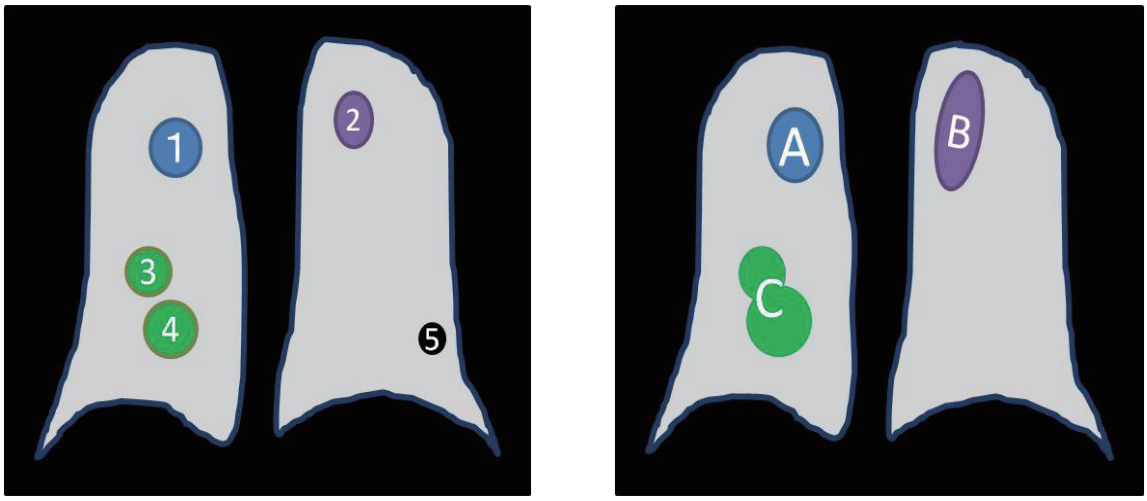

(a) I_a (b) I_b

Figure 4.4: Examples of two CT images for nodule matching. The nodule "1" in I_a should match to the nodule "A" in I_b. The nodules "3" and "4" in I_a should integrate and match to the nodule "C" in I_b.

The previous nodule matching method [158] only used the coordinates of the centroids of two nodules to measure their similarity. However, if an FP in a past (current) CT image is located near an actual nodule in a current (past) CT image, the false matching might easily occur only considering their positions. By utilizing the features of $\mathbf{d}$ and $\mathbf{I}$, although an actual nodule and a FP are located closely in two CT images, if their sizes and average intensities are differ completely, they will not be considered as corresponding nodules. The nodule "2" in Fig. 4.4(a) and the nodule "B" in Fig. 4.4(b) show an example of this case. Suppose to match the nodules $i(i = 1, .., M)$ in CT image I_a to nodules $j(j = 1, .., N)$ in another CT image I_b, M and N are the numbers of segmented nodules from I_a and I_b, respectively. We assign the coordinates of the centroids of nodules i and j as $\mathbf{g}_i^a$ and $\mathbf{g}_j^b$, respectively. Other features including diameter and average intensity are assigned as vectors $\mathbf{f}_i^{(a)} = [\mathbf{d}_i^{(a)}, \mathbf{I}_i^{(a)}]$ and $\mathbf{f}_j^{(b)} = [\mathbf{d}_j^{(b)}, \mathbf{I}_j^{(b)}]$, respectively. Then, the vectors $\mathbf{g}$ and $\mathbf{f}$ are combined as new high dimensional feature vectors $\mathbf{n}_i^{(a)} = [\mathbf{g}_i^{(a)}, \mathbf{f}_i^{(a)}]$ and $\mathbf{n}_j^{(b)} = [\mathbf{g}_j^{(b)}, \mathbf{f}_j^{(b)}]$. A feature vector space Ω is constructed using the feature vectors $\mathbf{n}$ of all the segmented nodule candidates. Then, the similarity of two nodules i and j are measured by the distance of their feature vectors in the space Ω.

Since the feature vector $\mathbf{n}$ consists of two components including the coordinate of

centroid and the features $\mathbf{f}$, we define the distance measure as

$$A = \begin{bmatrix} I & 0 \\ 0 & \omega\Sigma \end{bmatrix}, \tag{4.1}$$

where I is a 3×3 identity matrix. This matrix is used to calculate the distance of the centroids of two nodules. Σ is a covariance matrix of the feature vectors $\mathbf{f}$ in Ω, which is calculated by

$$\Sigma = \frac{1}{M+N}\left(\sum_{i=1}^{N}(\mathbf{f}_i^{(a)} - \boldsymbol{\mu})(\mathbf{f}_i^{(a)} - \boldsymbol{\mu})^T + \sum_{j=1}^{M}(\mathbf{f}_j^{(b)} - \boldsymbol{\mu})(\mathbf{f}_j^{(b)} - \boldsymbol{\mu})^T\right), \tag{4.2}$$

where $\boldsymbol{\mu}$ indicates the mean of the feature vectors $\mathbf{f}$ in Ω. $\boldsymbol{\mu}$ is calculated by

$$\boldsymbol{\mu} = \frac{1}{M+N}\left(\sum_{i=1}^{N}\mathbf{f}_i^{(a)} + \sum_{j=1}^{\mathbf{M}}\mathbf{f}_j^{(b)}\right). \tag{4.3}$$

$\omega(0 < \omega < 1)$ is a parameter that is utilized to control the magnitude of the distance measure. Then, the distance of the two nodules (i and j) on the feature vector space Ω can be calculated as

$$d(i,j) = (\mathbf{n}_i^{(a)} - \mathbf{n}_j^{(b)})^T A^{-1}(\mathbf{n}_i^{(a)} - \mathbf{n}_j^{(b)}). \tag{4.4}$$

If nodules i and j are corresponding nodules, then the distance $d(i,j)$ decreases in size. Hence, this distance can be utilized as a similarity measure of two nodules.

4.2.4.2 Similarity calculation patterns

We calculate the similarity of nodules $i(i = 1, .., M)$ in image I_a and the nodules $j(j = 1, .., N)$ in image I_b. To match the nodules with temporal changes in follow-up CT images, we consider three patterns for similarity calculations. The first pattern is the similarity calculation between two nodules from two CT images ($Pattern\ 1$: 1 to 1) (Fig. 4.5). This pattern corresponds to the most common matching pattern of two nodules. The second pattern in terms of the similarity calculation between one merged nodule in scan I_a and another nodule in scan I_b ($Pattern\ 2$: 2 to 1) (Fig. 4.6). We aim to match

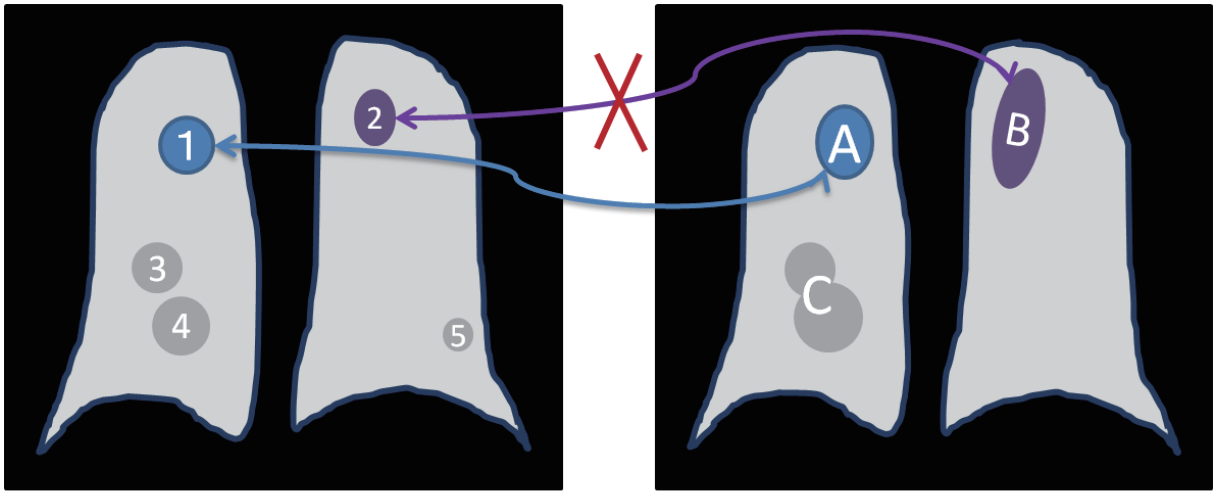

(a) I_a (a) I_b

Figure 4.5: Illustration of matching pattern 1. Nodule "1" in image I_a matches nodule "A" in image I_b. However, although nodule "2" and nodule "B" exist nearly, they will not be considered as corresponding nodules, since their shapes are differ completely.

the merged/separated nodules by this pattern. $Pattern\ 3$ aims to find nodules which do not have a match (non-corresponding nodule). This is in terms of the matching of appeared or disappeared nodules. As shown in figure 4.7, since the nodule "5" in I_a disappeared in I_b, nodule "5" is considered as a non-corresponding nodule. The details of these three matching patterns of similarity calculations are described as follows:

$Pattern\ 1$ **[1 to 1]**.

The likelihood of nodule i in image I_a and nodule j in image I_b to be corresponding nodules depends on their distance $d(i, j)$. The nodule "1" in Fig. 4.5(a) and the nodules "A" in Fig. 4.5(b) may be the corresponding nodules since they have small distance $d(1, A)$. Although the nodules "2" and "B" are located closely, their shapes are completely different. This causes the feature vectors $\mathbf{f}$ of nodules "2" and "B" to be very different, so that the distance $d(2, B)$ increases. Hence, nodules "2" and "B" will not be considered as corresponding nodules. We calculate the similarity

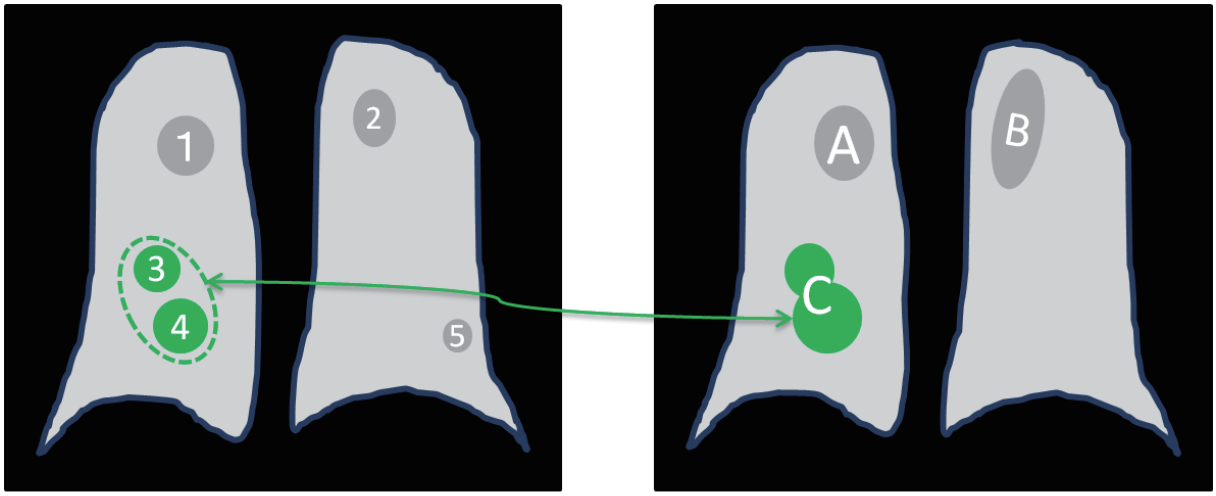

(a) I_a (a) I_b

Figure 4.6: Illustration of matching $Pattern\ 2$. The nodule "3" and "4" in image I_a merge together and match to the nodule "B" in image I_b.

$p(i,j)$ of each pair of nodules from two CT images by the equation:

$$p(i,j) = \frac{1}{(2\pi)^{\frac{d_{\mathbf{f}}+3}{2}}|A|^{\frac{1}{2}}} \times \exp\left[-\frac{1}{2}d(i,j)\right]. \tag{4.5}$$

This equation is defined following Gaussian distribution, where $d_{\mathbf{f}}$ indicates the number of dimensions of feature vector $\mathbf{f}$,

Pattern 2 **[2 to 1]**.

Due to nodule growth or the effect of treatment, some nodules merge together to become one nodule, or one nodule may separate to become two nodules in progress. Figure 4.6 illustrates this pattern. The nodule "3", "4" in I_a merge together and match to the nodule "B" in I_b. In order to describe such case, we combine two nodules i_1 and i_2 in image I_a to be a new nodule i, and calculate the feature vector $\mathbf{n}_i^{(I_a)} = [\mathbf{g}_i^{(I_a)}, \mathbf{f}_i^{(I_a)}]$ of this consolidated nodule i. Then, the similarity of nodule i and another nodule j in image I_b is calculated by the Eq. (4.5).

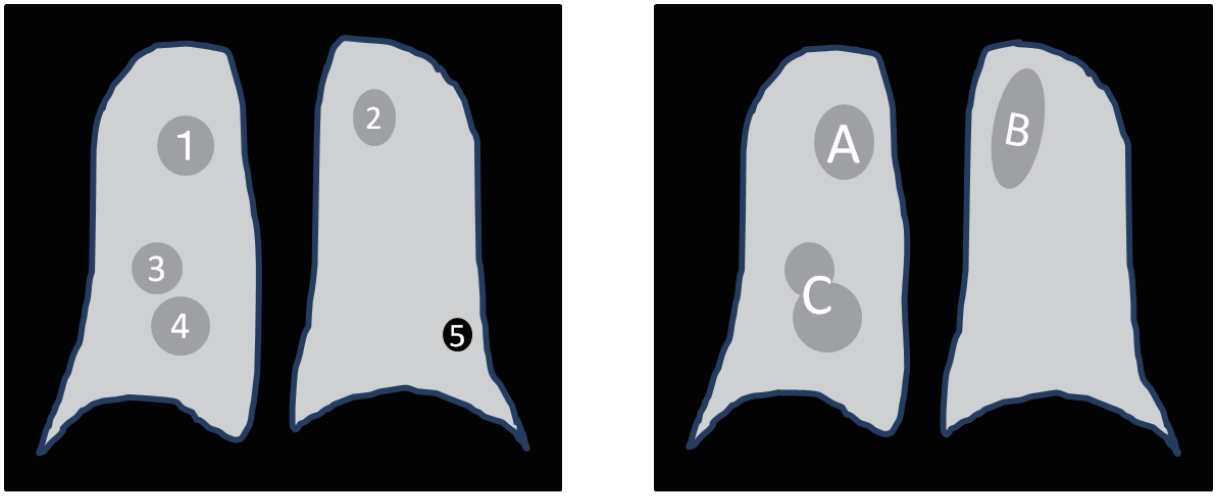

(a) I_a (a) I_b

Figure 4.7: Illustration of matching $Pattern\ 3$. The nodule "5"in image I_a has no corresponding nodule in I_b, which is considered as non-corresponding nodule.

$Pattern\ 3$ **[non-corresponding nodule]**.

Due to metastasis or the effect of treatment, the appearance and disappearance of a nodule may occur. Hence, a nodule in the current CT image may have no corresponding nodule in another CT image. We consider such nodule as a non-corresponding nodule (see the nodule "5" in Fig. 4.7). To investigate whether a nodule i is a non-corresponding nodule, the similarity of nodule i and the appeared/disappeared nodules is calculated. Since the appeared/disappeared nodule usually has a small volume, we choose the 5 smallest nodules from all of the segmented nodules of a patient as the appeared/disappeared nodules: $S_k(k = 1, ..., 5)$. In this pattern, only the feature vector $\mathbf{f}$ (without the g) is utilized to calculate the similarity measure as

$$p(i, S_k) = P_{isolate} \frac{1}{(2\pi)^{\frac{d_\mathbf{f}}{2}} |r\Sigma|^{\frac{1}{2}}} \times \exp\left[-\frac{1}{2}(\mathbf{f}_i^{(I_a)} - \mathbf{f}_s)^T (r\Sigma)^{-1} (\mathbf{f}_i^{(I_a)} - \mathbf{f}_s)\right], \tag{4.6}$$

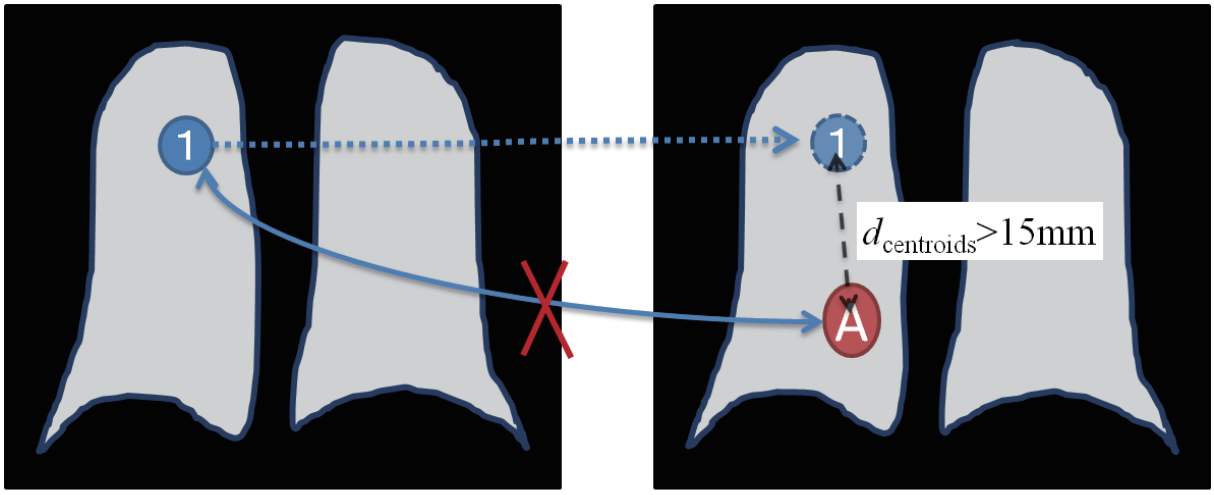

Figure 4.8: Illustration of $Constraint\ 1$. The distance between centroids of nodule "1" in image I_a and nodule "A" in image I_b is larger than $15mm$. The similarity calculation of these two nodules is skipped.

where $P_{isolate}$ is a weight parameter. Since the appearance and disappearance of nodules rarely occurs, $P_{isolate}$ is used to make the likelihood of $p(i, S_k)$ smaller than $p(i, j)$ (in Eq. (4.5)). In this case, the position of nodules is not used for similarity calculations. Hence, we utilize $r\Sigma$ instead of A as the distance measure, and $r(0 < r < 1)$ is a parameter. The vector $\mathbf{f}_s$ indicates the average feature vector $\mathbf{f}$ calculated from the small nodules S_k. $p(i, S_k)$ indicates the likelihood of nodule "i" whether is a non-corresponding nodule.

4.2.4.3 Constraints of similarity calculations

During the similarity calculation, if we consider the above three patterns for all of the nodules $i(i = 1, .., M)$ in I_a and nodules $j(j = 1, .., N)$ in I_b, a large number of impossible patterns of similarity calculation may be executed. This is time consuming and may lead to an insufficient matching result. To avoid the inadequate calculations, we implement three constraints for similarity calculations.

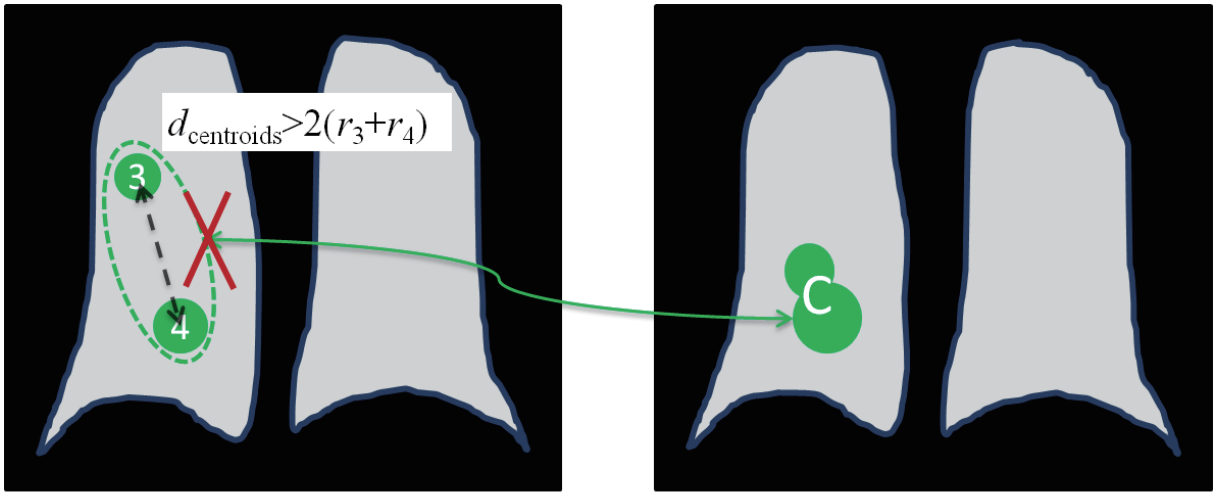

Figure 4.9: Illustration of $Constraint\ 2$. The distance between centroids of nodules "3" and "4" in image I_a is apparently lager than the sum of their radius. These two nodules are not considered to merge together and match to the nodule "C" in another image.

$Constraint\ 1$ **[Constraint for** $Pattern\ 1$ **]**

If the distance between the centroids of nodule i in I_a and j in I_b is very large, they should not be a pair of corresponding nodules. Figure 4.8 illustrates an example of this case. The distance of nodule "1" and nodule "A" is too large, the similarity calculation of them will be skipped. Hence, we only calculate the similarity of nodules i and j, which satisfy the following equation:

$$d_{centroids}(i,j) = (\mathbf{g}_i^{(a)} - \mathbf{g}_j^{(b)})^T(\mathbf{g}_i^{(a)} - \mathbf{g}_j^{(b)}) < 15[mm], \tag{4.7}$$

where $d_{centroids}(i,j)$ indicates the distance between centroids of nodule i and nodule j.

$Constraint\ 2$ **[Constraint for** $Pattern\ 2$ **]**

Generally, $Pattern\ 1$ [1 to 1] is the most common pattern for nodule matching. Only if two nodules are located closely in a CT image, they may merge together to become one nodule (or separated from one nodule) in another CT image. Hence, for the nodules i_1 and i_2 in image I_a, if the distance between their centroids

($d_{centroids}(i_1, i_2)$) is apparently larger than the sum of their radii, we do not combine them and implement the similarity calculation of $Pattern\ 2$ of them (see the nodules "3" and "4" in Fig.4.9(a)). We only implement the similarity calculation $Pattern\ 2$ for two nodules in a same CT image that satisfy the following equation:

$$d_{centroids}(i_1, i_2) \leq 2(r_{i_1} + r_{i_2}), \tag{4.8}$$

where r_{i_1}, r_{i_2} indicate the radius of nodule i_1 and i_2 , respectively.

$Constraint\ 3$ **[Constraint for** $Pattern\ 3$ **]**

The generation of new nodules (appeared nodule) due to the growth and the elimination of nodules (disappeared nodule) due to the effects of treatment do not occur in every CT image. We assume that the possible existence of such appeared/disappeared nodules depends on the change rate of the nodule numbers of two CT images. If the numbers of segmented nodules from images I_a and I_b are similar, then the possible existence of appeared or disappeared nodules may be close to 0. In the case of no appeared or disappeared nodules occurring in CT image, the calculation of pattern 3 may incorrectly determine a small nodule which has a corresponding nodule to be a non-corresponding nodule. Here, we only apply the similarity calculation of $Pattern\ 3$ when the change rate γ of the nodules in two CT images satisfies

$$\gamma = |N_{I_b} - N_{I_a}|/(N_{I_a} + 1) > \beta. \tag{4.9}$$

N_{I_a} and N_{I_b} indicate the number of nodules that segmented from image I_a and image I_b, respectively. β is a threshold value .

By implementing the above three constraints, the similarity calculation can be performed much more effectively and correctly.

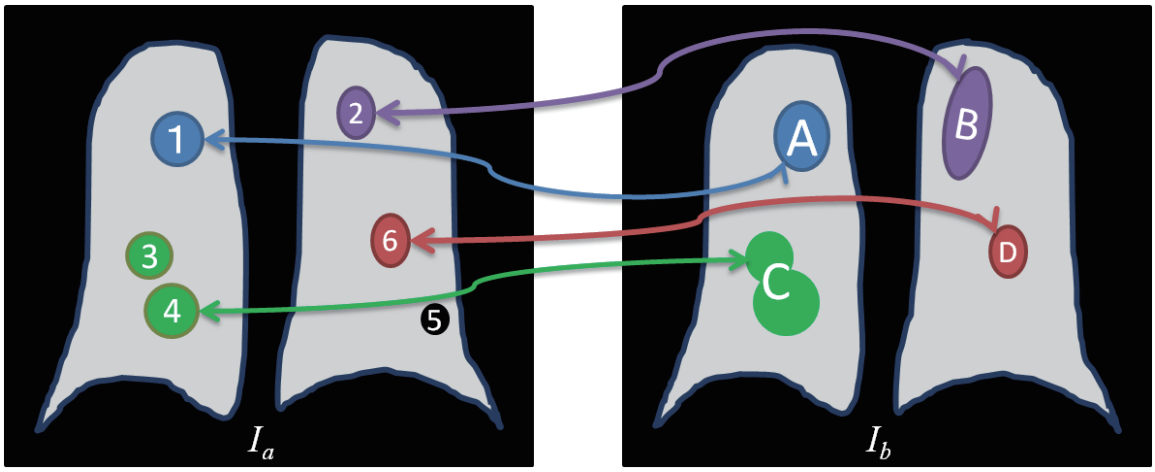

(a) Matching combination 1

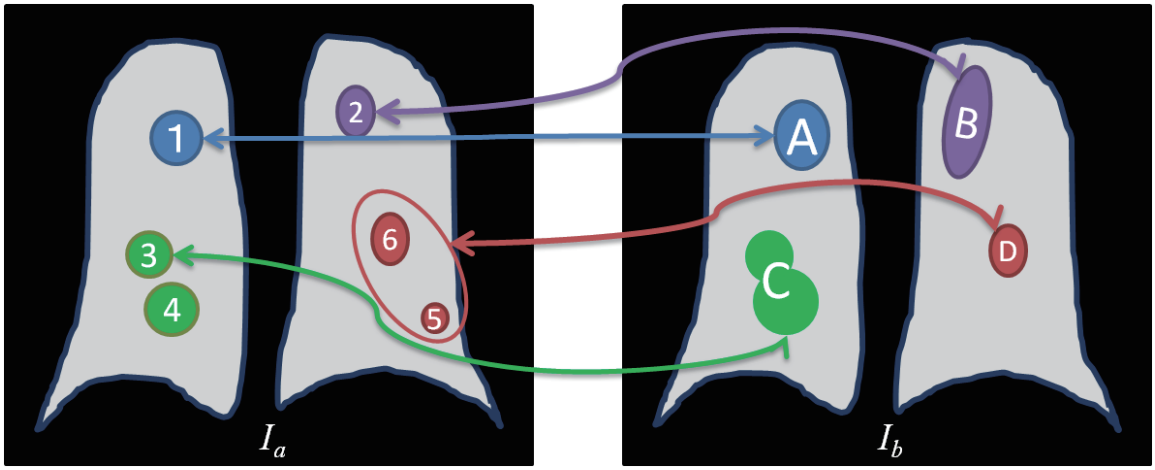

(b) Matching combination 2

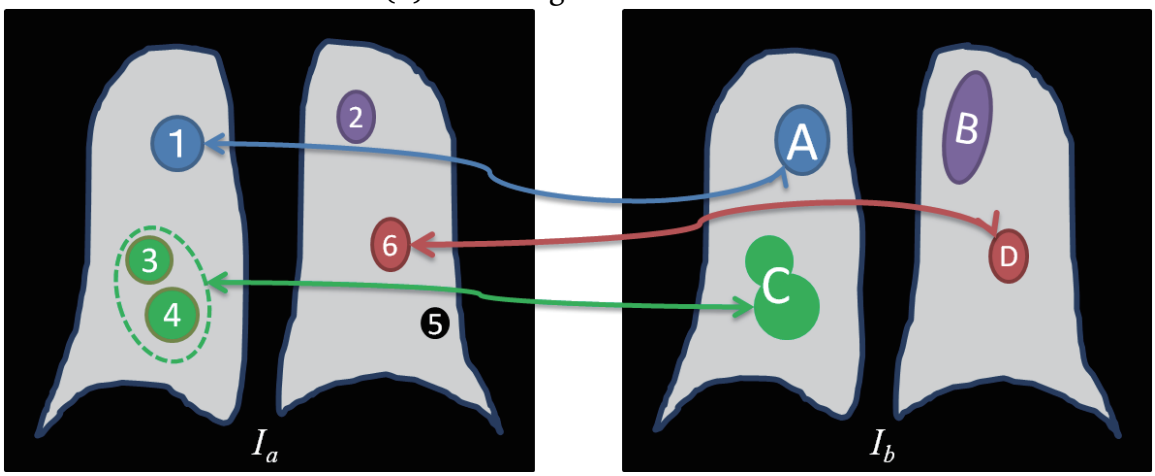

(c) Matching combination 3

Figure 4.10: Examples of matching combinations. Combination 3 (Fig. 4.10(c)) is considered as the matching results of I_a and I_b.

4.2.5 Corresponding nodule finding

After the similarity calculation for nodules i in image I_a and nodule j in image I_b, we combine every matching pattern and obtain a number of matching combinations. Every matching combination has a matching likelihood that is obtained from the similarity calculation. Figure 4.10 shows several examples of matching combinations of two CT images. The final nodule matching result is found as the matching combination which has a maximum likelihood.

Suppose the matching candidates of nodule i in image I_a are $j_i^{(t)}(j_i^{(t)} = 0, 1, 2..., S_k)$ and the matching candidates of nodule j in image I_b are $i_j^{(t)}(i_j^{(t)} = 0, 1, 2..., S_k)$, the likelihood $P(t)$ of combination t can be calculated as

$$P(t) = \prod_{i=1}^{N} p(i, j_i^{(t)}) * \prod_{j=1}^{M} p(i_j^{(t)}, j), \tag{4.10}$$

where $p(i, j)$ is the similarity between the nodules i and j. However, in the case of ($i = i_j^{(t)}$ and $j = j_i^{(t)}$), we only calculate $p(i, j_i^{(t)})$ to avoid the repetition of calculation. The combination which has the maximum likelihood will be selected as the final matching result. In Fig. 4.10, the combination 3 (shown in Fig. 4.10(c)) may have the maximum likelihood, and will be considered as the matching result of I_a and I_b.

Finally, we assign an unique ID to each pair of corresponding nodules. The same matching process is implemented to every two CT images for a patient.

4.3 Experiment and results

4.3.1 Materials and parameter estimation

We tested the proposed methods by using the chest CT images of three patients. These three serials of CT images include $8(A), 4(B)$,and $2(C)$ follow-up CT images, respectively. The acquisition parameters of CT images are shown in Table 4.1. The ground truth data of the nodule segmentation and matching were identified by physicians. In the ground truth data, 216 small lung nodules with diameters from $3.75[mm]$ to $27[mm]$

Table 4.1: Acquisition parameters of chest CT images

Image size	512×512	voxels
Number of slices	$185 - 246$	slices
Pixel spacing	$0.523 - 0.684$	mm
Slice spacing	1.25	mm
Slice thickness	2.5	mm

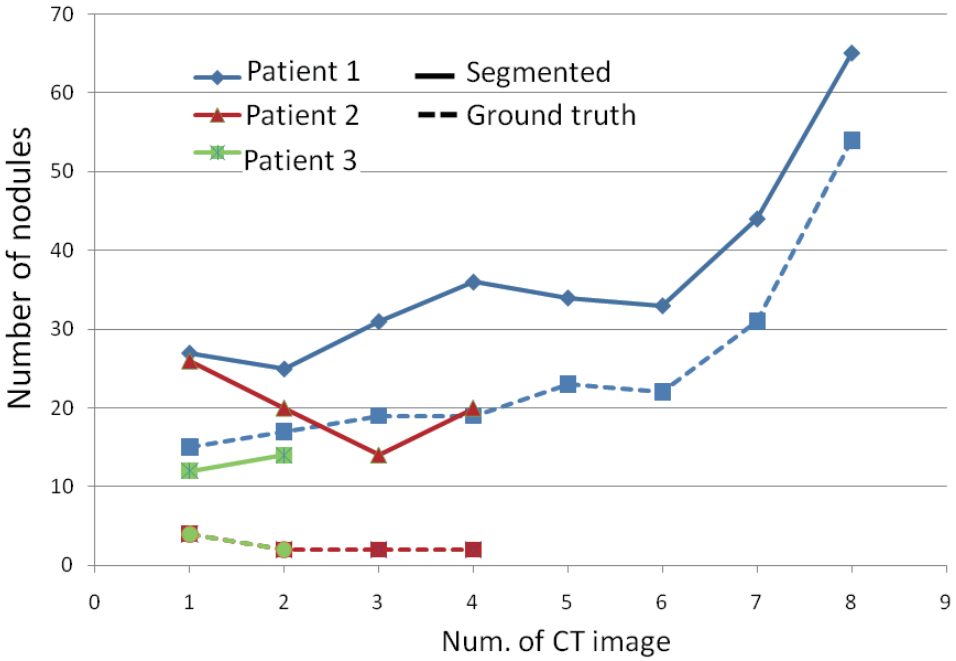

Figure 4.11: Change of the numbers of nodule in follow-up CT images of three patients.

were identified. Our automated nodule segmentation method (introduced in Chapter 3) detected $95.8\%(207/216)$ nodules with about 15 FPs per case. 37 "same nodule groups" (174 in individual) were found from the detected 207 nodules by physicians. The "same nodule group" means a group of matching nodules along all the CT images of a patient, but not only from two follow-up CT images. However, due to the appearance and disappearance, there is no guarantee that a corresponding nodule in a "same nodule group" occurs in the all CT images of a patient. Among these 37 "same nodule group" groups, 3 groups include the merged nodules. The appeared or disappeared nodules were found from every two follow-up CT images. The curves in Fig. 4.11 shows

Table 4.2: The nodule matching results of the proposed method

Method	Matching rate of merged nodule	False matched (group)	Missed matching (group)	Matching rate
Proposed $with\ \beta = 0.2$	100% (3/3)	1	1	94.6% (35/37)

the number of nodules of each CT image of these three patients. The straight lines and dashed lines indicate the nodule numbers obtained from the ground truth data and automatic segmentation results, respectively. Figure 4.11 demonstrate that two follow-up CT images may have the same number of nodules, the appeared or disappeared nodules do not occur in such cases. We found 102 appeared/disappeared nodules candidates from the automatic segmentation results of all the 14 CT images. However, only 45 appeared/disappeared nodule candidates were actual nodules, the others were FPs.

To evaluate the matching results, we computed the matching rate as

$$\text{Matching rate} = \frac{N_{Matched}}{N_{All}(=37)}, \tag{4.11}$$

where $N_{Matched}$ indicates the number of correctly matched "same nodule groups" by the proposed method, and N_{All} indicates all the 37 "same nodule groups". The proposed method obtained the best results as 94.6% (35 groups /37groups) matching rate with all the merged nodules matched correctly, when setting the parameters as : $P = 0.05$, $r = 0.25,\ w = 0.1$, $\beta = 0.2$ (Table 4.2). Figure 4.12 shows some examples of successfully matched nodules. Figure 4.12 (a) and (b) show two corresponding nodules that were matched by $Pattern\ 1$, Figure 4.12 (c) shows an example of merged nodules that was matched by $Pattern\ 2$. Figure 4.13 shows three examples of correctly matched nodules in the view of volume rendering.

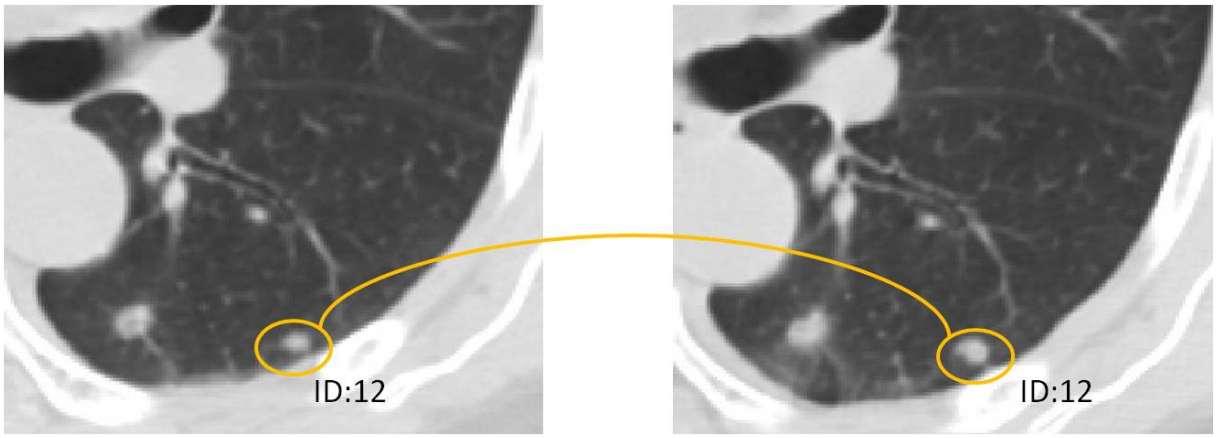

(a)

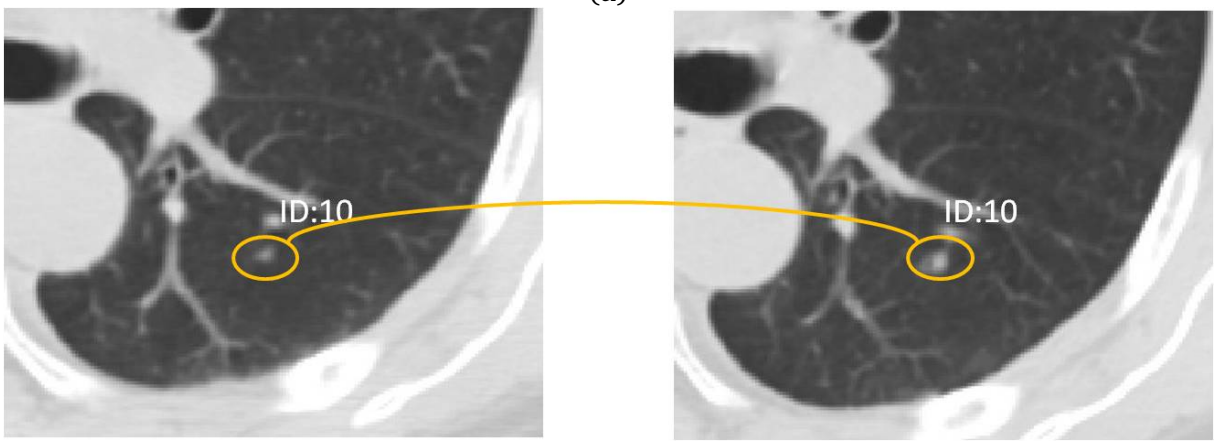

(b)

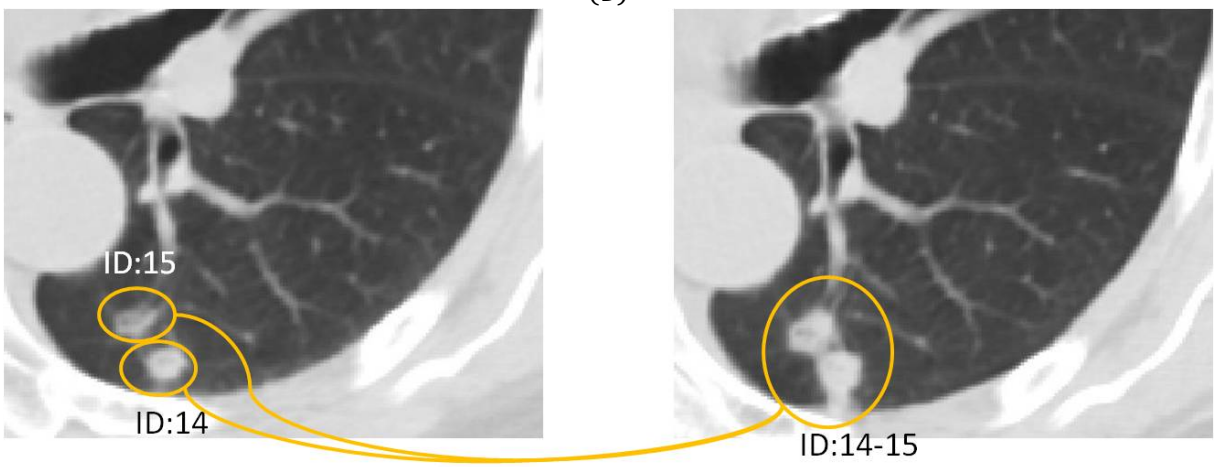

(c)

Figure 4.12: Examples of matching results. (a) and (b) show the examples of two normal corresponding nodules that are matched by $Pattern\ 1$, and (c) shows an example of merged nodules that are matched by $Pattern\ 2$. The nodules in the left image are combined and match to the nodule in the right image.

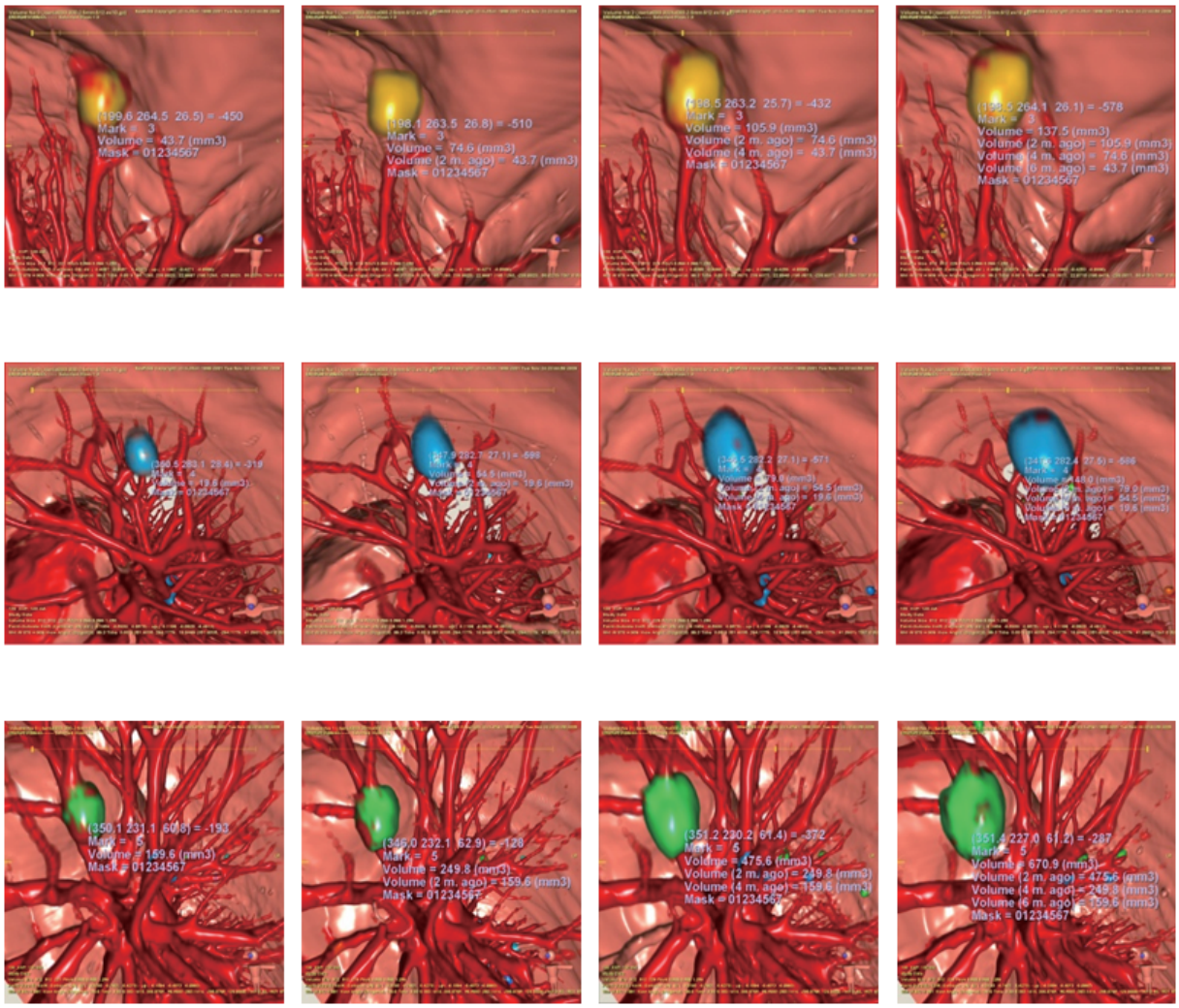

Figure 4.13: The examples of correctly matched nodules shown by volume rendering on follow-up CT images.

Table 4.3: Comparison of the proposed nodule matching method to the previous method

Method	Matching rate of merged nodule	False matched (group)	Missed matching (group)	Matching rate
Proposed $with\ \beta = 0.2$	100% (3/3)	1	1	94.6% (35/37)
Previous ([158])	0% (0/3)	5	2	81.1% (30/37)

4.3.2 Comparison with previous methods

Table 4.3 summarizes the comparison results of the proposed method and the previous method [158] using the same CT images. The previous method obtained 81.1% (30 groups/37 groups) matching rate, and failed to match all the merged corresponding nodules (Table 4.3). Since the previous automated nodule matching methods [154, 157, 159] have not reported the matching rate, we cannot compare the performances of these methods and the proposed method directly. The semi-automated method proposed by Cheng et al. [150] reported a 92.7% matching rate. However, this method belongs to Category 1 and requires the manually detection of nodules by mouse click. Since all of these previous methods only aim to find the corresponding nodules of $Pattern\ 1$ ([1 to 1]), these methods are limited to match the nodules without temporal changes. Furthermore, they were only tested for matching the actual nodules without FPs.

4.4 Discussion

4.4.1 Effectiveness of proposed method on reducing false matching

As shown in Table 4.3, the proposed method significantly improved the matching rate of nodules from the previous method [158]. The main reason for this improvement is in terms of the reduction of false matching.

(1) The previous method [158] utilized only the coordinate of centroid of a nodule as the feature vector and considered only a single matching pattern ($Pattern\ 1$) for similarity measurement. However, if an actual nodule and a FP are located closely in two follow-up CT images, only consider the position of their centroids for matching may cause the false matching of them. The proposed method additionally considers the diameter and average intensity values of nodule candidates to avoid such false matching. Although an actual nodule and an FP may be lo-

Table 4.4: Comparison of the proposed nodule matching methods to the method without the consideration of $Pattern\ 3$

Method	Matching rate of merged nodule	False matched (group)	Missed matching (group)	Matching rate
Proposed $with\ \beta = 0.2$	100% (3/3)	1	1	94.6% (35/37)
Proposed $without$ $Pattern\ 3$	100% (3/3)	4	1	86.5% (32/37)

cate closely, if their sizes and average intensities differ completely, they will not be considered as a pair of corresponding nodules.

(2) To match nodules that have temporal changes due to their growth or the effect of treatment, the proposed method considered three patterns for similarity measuring. This enables us to match the temporally changed nodules such as merged, separated or appeared, disappeared nodules. Particularly we implemented the similarity calculation of $Pattern\ 3$ to match the appeared/disappeared nodules (non-corresponding nodules), and correctly recognized all of the 45 non-corresponding nodules. This can avoid such non-corresponding nodules to be matched to the FPs incorrectly. The matching results of the proposed methods without the implementation of $Pattern\ 3$ are shown in Table 4.4. The results show that without the similarity calculation of $Pattern\ 3$, the matching rate decreases significantly. These results confirmed that the consideration of $Pattern\ 3$ is necessary.

4.4.2 Effectiveness of the similarity calculation of $Pattern\ 2$

We implemented the similarity calculations of $Pattern\ 2$ to match the merged/separated nodules. Since the previous methods only consider the normal matching patterns ($Pattern\ 1$), all of the three merged nodules have not been recognized (Table 4.3).

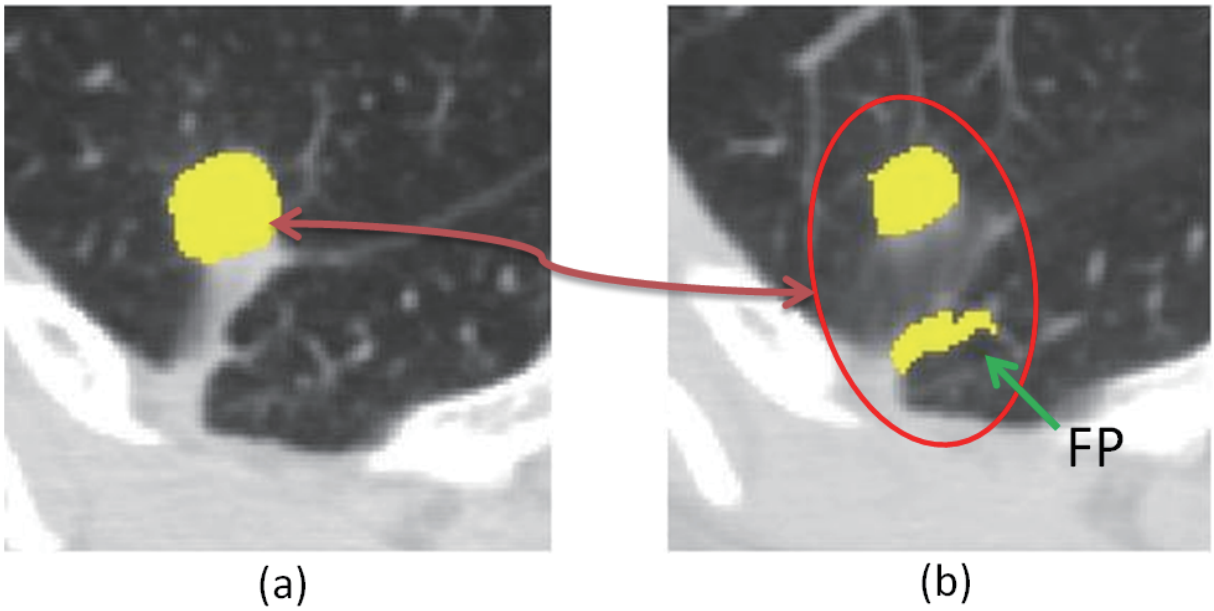

Figure 4.14: The false merged nodule. In the right image, a nodule was incorrectly merged with a FP. The merged nodule was considered to correspond to the nodule in the left image.

Two of these three merged nodules were incorrectly determined as non-corresponding nodules, another one was incorrectly matched to an FP. The proposed method correctly matched all the merged nodules by considering the similarity calculation of $Pattern\ 2$. However, one nodule was incorrectly merged with a FP (Fig. 4.14), and incorrectly matched to another nodule. This leads to false matching in the results shown in Table 4.3 and 4.4. To solve this problem, the implementation of a new constraint for the volume of merged nodule into $Pattern\ 2$ is considerable. This is because the volume of merged nodule is commonly larger than the nodules before merging.

4.4.3 Effectiveness of $Constraint\ 3$

The experimental results confirmed that the implementation of $Constraint\ 3$ is necessary (Table 4.5). In an early report of our research, we proposed a nodule matching method without the implementation of $Constraint\ 3$ (Chen et al. [160]). This previous method generated many missed corresponding nodules (see the results in Table 4.5:

Table 4.5: Comparison of the proposed nodule matching method to the method without consideration of $Constraint\ 3$

Method	Matching rate of merged nodule	False matched (group)	Missed matching (group)	Matching rate
Proposed *with* $\beta = 0.2$	100% (3/3)	1	1	94.6% (35/37)
Proposed *without* $Constraint\ 3$	100% (3/3)	1	5	83.8% (31/37)

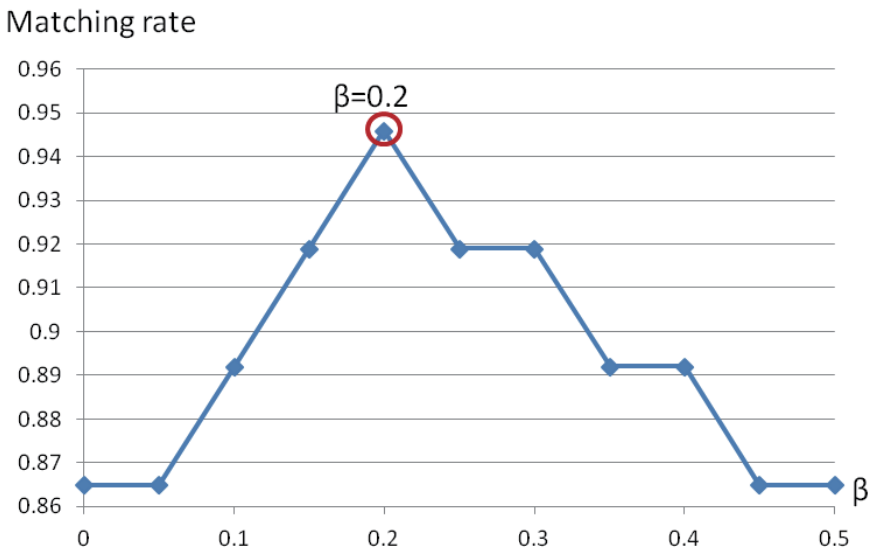

Figure 4.15: The change of matching rate with different settings of β. The best result was obtained when setting β to 0.2.

Proposed without $Constraint\ 3$).

The results in Fig. 4.11 confirmed that the generation of new nodules and the elimination of nodules does not occur in every CT image. In such cases, the calculation of $Pattern\ 3$ may incorrectly determine a small nodule which has a corresponding nodule to be a non-corresponding nodule. In the proposed method, we applied $Constraint\ 3$ for the similarity calculation of $Pattern\ 3$. Hence, the similarity calculation of $Pattern\ 3$ can only be implemented when the change rate γ of the nodule numbers segmented from

two follow-up CT images satisfies the Eq. (4.9). This significantly reduced the number of missed corresponding nodules, which confirmed that $Constraint\ 3$ is required (Table 4.5).

Figure 4.15 shows the different matching results obtained by the different settings of parameter β in the $Constraint\ 3$. The best result was obtained when $\beta = 0.2$.

4.4.4 Limitations

The automated nodule matching method proposed in this chapter provided good performance for finding corresponding nodules. The experimental results also confirmed that the proposed method is robust to the temporal changes of nodules. However, this method still has some limitations.

First, the performance of the proposed nodule matching method depends on the nodule segmentation results. Although the proposed method showed good performance for avoiding the false matching of an actual nodule and an FP, if the segmentation results includes too many FPs, the generation of such false matching may become unavoidable. On the other hand, the false negatives in the segmentation result cause the missed matching of proposed method.

Second, the implementation of $Constraint\ 3$ significantly reduced the generation of missed corresponding nodules. However, if the number of appeared nodules is same as the number of disappeared nodules in two CT images, then the change rate of the number of nodules becomes zero. In this case, the similarity calculation of $Pattern\ 3$ will be skipped because of $Constraint\ 3$. This may be because the proposed method cannot recognize the non-corresponding nodules.

Third, the existences of other lesions in lungs may potentially influence the matching performance. The lung lesions such as pneumonia and emphysema usually cause lung tissue to differ from normal lungs. This may decrease the registration accuracy of two CT images, and finally influence the nodule matching performance of the proposed method.

4.5 Conclusions

In this chapter, we have proposed a novel automated nodule matching method. The proposed method can automatically find the corresponding nodules for the nodules that are segmented from follow-up chest CT images.

To compensate for lung deformations the proposed method utilizes rigid registrations and a non-rigid registration processes to co-register follow-up CT images. By considering the temporal change of nodules, we implement three patterns for the similarity calculation of nodules. These three patterns correspond to the matching of normal nodules, the merged/separated nodules, and the appeared/disappeared nodules, respectively. The similarity calculation is based on the features including the position of centroids, diameter, and average intensity of nodules.

The experimental results confirmed that the proposed method is robust to temporal changes in nodules such as the appearance/disappearance or the merger/separation, and the proposed method significantly improved the performance of nodule matching from the previous methods. This enables clinicians to diagnosis nodules by the growth or assessing the effect of treatment on metastatic lung nodules.

Future work includes (1) further discussion of $Pattern\ 3$ to avoid the incorrect merger, and (2) evaluation by a large number of cases and different nodule segmentation results.

Chapter 5

Conclusions and future work

This chapter concludes the accomplishments that have been discussed in this dissertation. The benefits and limitations of the proposed methods are discussed in section 5.2. and we will also discuss some promising directions for future work to further address the development of the chest CAD system.

5.1 Summary

This dissertation introduced an automated segmentation method for both solitary pulmonary nodules (SPNs) and pulmonary vessels. An automated nodule matching method for assisting the observation of segmented lung nodules was also proposed. The functions derived from the proposed methods are integrated into our chest CAD system.

(1) This dissertation has described a Hessian and level set-based methodology for segmentation of both SPNs and vessels (Chapter 3). The proposed method incorporates the enhancement results of Hessian-based LSE and BSE filters into a level set scheme to improve the segmentation performance of both nodules and blood vessels. The previous nodule segmentation methods have good performance in detecting lung nodules, but usually generate many false positives (FPs). The main goal of the proposed method is to provide a low number of FPs per case while keeping high sensitivity. Since the FPs mainly occur in blood vessel regions in the

initial nodule candidate detection process, the key-point is how to discriminate between the blood vessels and nodules, especially the vessel-attached nodules. To deal with such problem, the proposed method incorporates the initial vessel regions and nodule candidates into the front surface propagation (FSP) procedure to make the front surface cover only the blood vessels with suppression of nodules. Consequently, the regions covered by the front surface are considered as pulmonary blood vessels, whereas the nodule detection result is obtained by removing nodule candidates covered by the front surface. The results using clinical chest CT images (40 CT images contains 416 SPNs) showed that the proposed method functions sufficiently in a chest CAD system.

(2) This dissertation has described a novel method for the automated matching of segmented nodules from follow-up chest CT images (Chapter 4). The proposed automated nodule matching method can handle the matching of nodules which display temporal changing, such as merged/separated nodules and appeared/disappeared nodules. By considering such temporal changes, the proposed method applied three patterns of similarity calculation, which are utilized to match the normal nodules, integrated/separated nodules, and appeared/ disappeared nodules, respectively. To compensate for both the inelastic and elastic deformations of follow-up CT images, the proposed method employed rigid registrations and improved non-rigid registration procedure. Furthermore, to avoid the incorrect matching of actual nodules and FPs existing closely in CT images, the proposed method also utilized the features of average intensities and diameters of nodules for the similarity measure in addition to position information. Consequently, two nodule candidates exist closely in CT images, they will not be considered as a matched pair if their features are totally different. By applying the proposed methods to 14 CT images, very promising nodule matching results were obtained.

5.2 Benefits and limitations

5.2.1 Benefits

(1) **Segmentation of SPNs and blood vessels:**

This work for the first time introduces a method that incorporates the enhancement results of Hessian-based LSE and BSE filters into a level set scheme to improve the segmentation performance of both nodules and blood vessels. The proposed method can finely separate and segment the SPNs and pulmonary blood vessels from chest CT images. This enables us to perform further analysis of lung nodules and vessels, such as matched nodules finding, the analysis of the relation of nodules and vessels. Also, the segmentation results can be utilized to perform the surgical navigation. The medical image processing techniques of segmentation that are developed in this dissertation can be applied to other CAD systems for the segmentation of tumors, vasculatures, and organs such as liver tumors, vessels, and airways.

(2) **Nodule matching:**

This work for the first time introduces a nodule matching method that can address the matching of temporarily changed nodules, such as merged/separated nodules and appeared/disappeared nodules. The experimental results confirmed that the proposed nodule matching method has a good performance in finding corresponding nodules, and is robust enough to handle the temporal changes in nodules. This enables the further analysis of lung nodules, such as malignancy analysis of lung nodule, effect analysis of treatment based on the nodule growth. Also, the matching results can be utilized to assist various clinical applications, such as surgical planning, therapy planning and treatment. The techniques of nodule matching developed in this dissertation can be applied to match and observe the other tumors and structures such as liver tumors, lymph nodes, and so on.

5.2.2 Potential limitations

Although the proposed methods introduced in this dissertation provide various significant improvements over previous methods, both the segmentation method and matching method have their own limitations.

5.2.2.1 Limitations of segmentations

The proposed segmentation methods have three main limitations as follows:

(1) The performance of nodule segmentation depends on the pulmonary vessel segmentation results, and vice versa. The proposed segmentation method aims to improve the segmentation accuracies of both SPNs and blood vessels by incorporating the information of their initial segmentation results. However, if the segmentation of blood vessels fails, the accuracy of nodule segmentation declines.

(2) The performance of both pulmonary nodule segmentation and blood vessel segmentation depends on the lung extraction accuracy. Since the segmentation procedures are applied inside the lung areas, the segmentation results of SPNs and blood vessels will worsen if lung extraction result is insufficient.

(3) The proposed nodule segmentation method is unable to reduce the number of FPs that are generated in other organs such as bones, chest walls, cardiac area. Since the proposed method focuses on separating the nodules and blood vessels to improve the segmentation performance, the FPs generated in blood vessel regions can be removed. However, several FPs may occur at the bones, chest walls and cardiac region. The proposed method cannot reduce such FPs.

5.2.2.2 Limitations of nodule matching

The proposed nodule matching method have several potential limitations as follows:

(1) The performance of nodule matching method depends on the segmentation results. Although the proposed method has good performance in reducing the false

matching of an actual nodule and an FP, if the segmentation results includes too many FPs, the generation of such false matching may become unavoidable. On the other hand, the false negative in the segmentation result may cause the missed matching of the proposed method.

(2) If the number of appeared nodules is equal to the number of disappeared nodules in two CT images, the change rate of the number of nodules may become zero. In this case, the similarity calculation of $Pattern\ 3$ (See section 4.2.4.3) will be skipped. This causes the proposed method to be unable to recognize the non-corresponding nodules, so that finally leads to the decreasing of nodule matching rate.

(3) The existences of other lesions in the lungs may potentially influence matching performance. The other lung lesions such as pneumonia and emphysema usually causes lung tissue differ from normal lungs. This may decrease the registration accuracy of two CT images, and finally influence the nodule matching result.

5.3 Future work

5.3.1 Improvement of proposed methods

To solve the limitations described in section 5.2.2, we discuss several promising ideas in the following:

(1) **Improvement of lung extraction:**

Both the proposed segmentation and matching methods have to extract lungs from input chest CT images as a preprocessing. Their performances depend on the extraction accuracy of the lungs. The current lung extraction method [142] is widely used for the rough extraction of lungs, but usually insufficient to extract the edges of the lungs near the chest walls and hilar. Utilization of some precise structure extraction methods such as graph cuts-based method, level set-based method may be the good solution for such problem.

(2) **Reduction of the FPs at non-vessel regions of the nodule detection method:**
One of the approaches to reduce the FPs generated at non-vessel regions such as the chest wall and other cardiac regions is to improve the extraction accuracy of thelungs, which was presented above. Other solutions may focus on the further reduction of FPs. Utilization of the feature-based machine learning approach or observation of neighborhood regions of nodule candidates may be sensitive.

(3) **Development of a neighborhood features-based FP reduction method:**
Since the performance of our proposed nodule segmentation method depends on blood vessel segmentation, development of a much more robust method is required. By observing the neighborhood regions of an actual nodule and an FP, we found that they show totally different profiles. To develop a neighborhood features-based FP reduction method is desirable.

(4) **Precise segmentation of nodule margins:**
The proposed method can segment the nodule regions finely. However, in order to perform the further analysis of nodules, such as the observation of growth rate, the analysis of malignancy, the precise segmentation of nodule margin regions is required. Such precise segmentation can be performed by level set-based methods, water shade-based methods, and so on.

(5) **Validation of the proposed methods by a large chest CT database:**
Although the proposed methods in this dissertation provides significant improvements over the current methods, further validations by using a larger database are required. The new experiment results would represent some new problems of proposed methods, as well as provide new solutions for current problems.

5.3.2 Further development of chest CAD system

For a chest CAD systems, which focus on the computer aided detection and diagnosis of lung nodule (or lung cancer), the automated segmentations of lung nodules, lung tissues (blood vessels) and automated nodule matching are very important. However,

the development of a state-of-the-art chest CAD system, several other functions are also required.

(1) **Segmentation of Ground Glass Opacity (GGO):**
Some researches have suggested that the GGO are more likely to be malignant than the solitary nodule [163]. Hence, to segment and analyze the GGO in the chest CT image is required for a chest CAD system.

(2) **Classification and labeling of pulmonary blood vessels:**
The relation of the nodules and blood vessels provides very useful information for the diagnosis of lung cancer. Benign lung nodules can be caused by blood vessel abnormalities. Different types of lung cancer may attach to different pulmonary vessels (e.g.,the adenocarcinoma is usually observed attaches to pulmonary vein). Furthermore, to understand the anatomic name of the blood vessels that locate near the lung cancer is important during the surgery. Hence, the classification of the pulmonary artery and vein, the labeling of each vessel branch are desirable for the aided diagnosis of lung cancer.

(3) **Malignancy analysis of nodule:**
Malignancy analysis of lung nodule is very important in the diagnosis of lung cancer. By the observation of nodules in CT image, the malignant likely nodule will be further diagnosed via biopsy. The nodules that are likely benign will be observed in follow-up CT images, and the ones that have not changed over a period of a few yeas can be left alone. CAD system that can support the malignancy analysis of nodule is desirable for lightening the burden of radiologists. Generally,to analyze the shape, opacity and growth of nodules may provide several advices for the malignancy analysis.

(4) **Quantitative analysis of the treatment effect for lung cancer:**
A chest CAD system that can provide the analysis results of treatment effect is required for treatment planning. Such analysis can be executed by considering

the relation of the growth, the treatment cycle, and the treatment step of lung cancer.

(5) **Metastatic situation analysis:**

Lung cancer tends to spread or metastasize very early, to analysis its metastatic situation is important. Since lung cancer usually spreads to the lymph nodes or through the bloodstream to other parts of body [15, 16] the automated segmentation and analysis of lymph nodes is a promising direction for understanding the metastatic situation.

5.3.3 Other applications

Although the main purpose of our system is to aid in the diagnosis of lung nodules (or lung cancer), to extent the functions of the developing system to the field of computer aided surgery (CAS) of lung cancer is also required.

During the lung cancer surgery, visualization of the lesions and lung tissues is helpful for the surgeon to perform the surgery much more efficiently and safely. Besides, during a bronchoscopy, to navigate the the doctors by visualizing the insertion path, the distance between lesions and the current position of the tip of bronchoscope are required. This can led to a smooth treatment, reducing the burden on physicians to perform the bronchoscopy, and reducing the burden on patients by shortening the time required for the bronchoscopy. The researches on the visual bronchoscopy and navigated bronchoscopy have been developed for a long period in our laboratory [164, 165, 166], and significantly improved in recent years [167, 168]. We confirm that a much more efficient and effective system can be developed by combining such researches and our developing chest CAD system.

In the future, we think our developed CAD system will be a multifunctional CAD system that can be used to diagnose a large number of target organs and diseases. We believe that our CAD system will be utilized by physicians to provide technical support during diagnosis and treatment. Also, in the absence of a doctor, our system will allows

for the automated identification and possible emergency treatment of life-threatening symptoms. These are quite important for the improvement of the quality of life (QOL) and make social contributions.

Bibliography

[1] K. Doi, “Computer-aided diagnosis in medical imaging: Historical review, current status and future Potential,” Computerized Medical Imaging and Graphics, 31(4-5):198-211, 2007.

[2] J. S. Tang, R. M. Rangayyan, J. Xu, I. E. Naqa, Y. Y. Yang, “Computer-aided detection and diagnosis of breast cancer with mammography: Recent advances,”IEEE Transactions on Information Technology in Biomedicine, 13(2):236-251, 2009.

[3] H. Yoshida, J. Nappi, “Three-dimensional computer-aided diagnosis scheme for detection of colonic polyps, ”IEEE Transactions on Medical Imaging, 20(12):1261-1274, 2001.

[4] Q. Li, “Recent progress in computer-aided diagnosis of lung nodules on thin-section CT,” Computerized Medical Imaging Graphics, 31(4-5): 248-257, 2007.

[5] J. B. West, “Respiratory physiology– the essentials,” Baltimore: Williams & Wilkins, 1-10, 2000.

[6] National Cancer Institute (NCI) at the National institutes of Health (NIH, US), “Metastatic cancer: Questions and answers,” NCI Fact Sheet, Retrieved 2011. [Online]
URL http://www.cancer.gov/cancertopics/factsheet/Sites-Types/metastatic

[7] National Cancer Institute (NCI) at the National institutes of Health (NIH, US), “What you need to know about^{TM} $LungCancer$,” NIH Publication, No. 07-1553,

2007. [Online]
URL http://www.cancer.gov/cancertopics/wyntk/lung

[8] World Health Organization, Cancer, Fact sheet N °297, 2011. [Online]
URL http://www.who.int/mediacentre/factsheets/fs297/en/index.html.

[9] M. C. Stoppler, "Lung cancer, causes, types, and treatment," retrieved from Medicine Net Inc., 2009. [Online]
URL http://www.medicinenet.com/lung_cancer, 2009.

[10] N. Howlader, A. M. Noone, M. Krapcho, N. Neyman, R. Aminou, W. Waldron, S. F. Altekruse, C. L. Kosary, J. Ruhl, Z. Tatalovich, H. Cho, A. Mariotto, M. P. Eisner, D. R. Lewis, H. S. Chen, E. J, Feuer, K. A. Cronin, B. K. Edwards (eds)., "SEER cancer statistics review," 1975-2008, National Cancer Institute, 2011.
URL http://seer.cancer.gov/csr/1975_2008/

[11] J. D. Minna, J. H. Schiller, "Harrison's principles of internal medicine (17th ed.)," McGraw-Hill, 551-562, 2008.

[12] B. B. Tan, K. R. Kazerooni, E. A. Kazerooni, M. D. Iannettoni, "The solitary pulmonary nodule," Chest, 123(1):89S-96S, 2003.

[13] W. I. Tuddenham, "Glossary of terms for thoracic radiology: recommendations of the nomenclature committee of the Fleischner Society," American Journal of Roentgenology, 143(3):509-517, 1984.

[14] S. J. Swensen, M. D. Silverstein, E. S. Edell, V. F. Trastek, G. L. Aughenbaugh, D. M. Ilstrup, C. D. Schleck, "Solitary pulmonary nodules: clinical prediction model versus physicians," Mayo Clinic Proceedings, 74(4):319-29, 1999.

[15] A. Vaporciyan, J. Nesbitt, L. Lee, "Cancer medicine," Hamilton (ON): B C Decker, 2000.

[16] CANCERcare, "Lung cancer 101: Screening & Early detection," lungcancer.org. [Online]
URL http://www.lungcancer.org/reading/screening.php.

[17] W. K. Hong, A. S. Tsao et al., "Lung carcinoma: Tumors of the lungs," Merck Manual Professional Edition, Online edition, Retrieved 2008. [Online]
URL http://www.merckmanuals.com/professional/pulmonary_disorders/tumors_of_the_lungs/lung_carcinoma.html

[18] O. Y. Gorlova, S. F. Weng, Y. Zhang, C. I. Amos, M. R. Spitz, "Aggregation of cancer among relatives of never-smoking lung cancer patients," International Journal of Cancer, 121(1):111-118. 2007.

[19] A. K. Hackshaw, M. R. Law, N. J. Wald, "The accumulated evidence on lung cancer and environmental tobacco smoke," British Medical Journal, 315(7114):980-988, 1997.

[20] O. Catelinois, A. Rogel, D. Laurier, S. Billon, D. Hemon, P. Verger, M. Tirmarche, "Lung cancer attributable to indoor radon exposure in France: impact of the risk models and uncertainty analysis," Environ Health Perspect, 114(9):1361-6, 2006.

[21] K. M. O'Reilly, A. M. Mclaughlin, W. S. Beckett, P. J. Sime, "Asbestos-related lung disease," American Family Physician, 75(5):683-688, 2007.

[22] Z. Kabir, K. Bennett, L. Clancy, "Lung cancer and urban air-pollution in dublin: a temporal association," Irish Medical Journal, 100(2):367-369, 2007.

[23] Y. M. Coyle, A. T. Minahjuddin, L. S. Hynan, J. D. Minna, "An ecological study of the association of metal air pollutants with lung cancer incidence in Texas," Journal of Thoracic Oncology, 1(7):654-661, 2006.

[24] Radiologyinfo.org, Radiological Society of North America (RSNA), American College of Radiology, "X-ray (radiography), chest: What is a chest X-ray (chest radio-

graphy)?" [Online]
URL http://www.radiologyinfo.org/en/info.cfm?pg=chestrad # part_one

[25] R. L. Manser, L. B. Irving, C. Stone, G. Byrnes, M. Abramson, D. Campbell, "Screening for lung cancer," Cochrane database of systematic reviews, (1):CD001991, 2004. [Online]

[26] B. L. Eldridge, "CT lung cancer screening: Issues to consider before having a CT scan to screen for lung cancer," About.com Guide, 2011

[27] A. Ernst, "Introduction to bronchoscopy." Cambridge University Press, 2009.

[28] Radiologyinfo.org, Radiological Society of North America (RSNA), American College of Radiology, "Needle biopsy of lung nodules" [Online]
URL http://www.radiologyinfo.org/en/info

[29] J. David, "Lung cancer treatment," Lung Cancer Answer. [Online]
URL http://www.lung-cancer.com/treatment.html

[30] W. A. Kalender, "Computed tomography: Fundamentals, system technology, image Quality, applications," Hoboken, NJ: Wiley, 2000.

[31] W. Robb, "Perspective on the first 10 years of the ct scanner industry," Academic Radiology, 10(7):756-760, 2003.

[32] J. H. Austin, N. L. Muller, P. J. Friedman, D. M. Hansell, D .P. Naidich, M. Remy-Jardin, W .R. Webb, E. A. Zerhouni, "Glossary of terms for CT of the lungs: recommendations of the Nomenclature Committee of the Fleischner Society," Radiology, 200(2):327-31, 1996.

[33] E. A. Zerhouni, J. F. Spivey, R. H. Morgan, F. P. Leo, F. P. Stitik, S. S. Siegelman, "Factors influencing quantitative CT measurements of solitary pulmonary nodules," Journal of Computer Assisted Tomography, 6(6):1075-1087, 1982.

[34] G. S. Lodwick, C. L. Haun, W. E. Smith, R. F. Keller, E. D. Robertson, "Computer diagnosis of primary bone tumor," Radiology, 80:273-5, 1963.

[35] P. H. Myers, C. M. Nice, H. C. Becker, W. J. Nettleton, J. W. Sweeney, G. R. Meckstroth, "Automated computer analysis of radiographic images," Radiology, 83:1029-33, 1964.

[36] F. Winsberg, M. Elkin, J. May, V. Bordaz, W. Weymouth, "Detection of radiographic abnormalities in mammograms by means of optical scanning and computer analysis," Radiology, 89:211-5, 1967.

[37] R. P. Kruger, J. R. Towns, D. L. Hall, S. J. Dwyer, G. S. Lodwick, "Automated radiographic diagnosis via feature extraction and classification of cardiac size and shape descriptors," IEEE Transactions on Biomedical Engineering, 19(3):174-86, 1972.

[38] J. Toriwaki, Y. Suenaga, T. Negoro, T. Fukumura, "Pattern recognition of chest x-ray images," Computer Graphics and Image Processing, 2:252-71, 1973.

[39] R. S. Fontana, D. R. Sanderson, W. F. Taylor, L. B. Woolner, W. E. Miller, J. R. Muhm, M. A. Uhlenhopp, "Early lung cancer detection: results of the initial (prevalence) radiologic and cytologic screening in the Mayo Clinic study," The American Review of Respiratory Disease, 130(4):561-565, 1984.

[40] M. L. Giger, K. T. Bae, H. MacMahon, "Computerized detection of pulmonary nodules in CT images," Investigative Radiology, 29(4):459-465, 1984.

[41] M. Kaneko, K. Eguchi, H. Ohmatsu, R. Kakinuma, T. Naruke, K. Suemasu, and N. Moriyama, "Peripheral lung cancer: Screening and detection with low-dose spiral CT versus radiography," Radiology, 201(3):798-802, 1996.

[42] M. L. Giger, Z. Huo, M. A. Kupinski, C. J. Vyborny, "Computer aided diagnosis in mammography," The handbook of medical imaging, 2:915-1004, 2000.

[43] B. J. Erickson, B. Bartholmai, "Computer-aided detection and diagnosis at the start of the third millennium," Journal of Digital Imaging, 15(2):59-68, 2002

[44] R. M. Summers, "Road maps for advancement of radiologic computer-aided detection in the 21st century," Radiology, 229(1):11-3, 2003.

[45] L. E. Dodd, R. F. Wagner, S. G. Armato, M. E. McNitt-Gray, S. Beiden, H-P. Chan, D. Gur, G. McLennan, C. E. Metz, N. Petrick, B. Sahiner, J. Sayre, the LIDC Research Group, "Assessment of methodologies and statistical issues for computer-aided diagnosis of lung nodules in computed tomography: contemporary research topics relevant to the lung image database consortium," Academic Radiology, 11(4):462-75, 2004.

[46] D. Gur, B. Zhang, C. R. Fuhrman, L. Hardesty, "On the testing and reporting of computer-aided detection results for lung cancer detection." Radiology, 232(1):5-6, 2004.

[47] I. Gori, M. E. Fantacci, A. P. Martinez, A. Retico, "An automated system for lung nodule detection in low-dose computed tomography," Proceedings of SPIE Medical Imaging, 6514:65143R, 2007

[48] K. Doi, "Current status and future potential of computer-aided diagnosis in medical imaging," British Journal of Radiology, 78(1):S3-s19, 2005.

[49] E. D. Pisano, C. A. Gatsonis, M. J. Yaffe, R. E. Hendrick, A. N. A. Tosteson, D. G. Fryback, L. W. Bassett, J. K. Baum, E. F. Conant, R. A. Jong, M. Rebner, C. J. D'Orsi, "American college of radiology imaging network digital mammographic imaging screening trial: Objectives and methodology," Radiology, 236(2):404-412, 2005.

[50] J. Wei, B. Sahiner, L. Hadjiiski, H. Chan, N. Petrick, M. Helvie, M. Roubidoux, J. Ge, and C. Zhou, "Computer aided detection of breast masses on full field digital mammograms," Medical Physics, 32(9):2827-2837, 2005.

[51] URL http://www.icadmed.com/products/mammography/secondlookdigital.htm

[52] URL http://www.kodak.com/go/mammo

[53] R. F. Brem, J. A. Rapelyea, G.Zisman, J. W. Hoffmeister, M. P. Desimio, "Evaluation of breast cancer with a computer-aided detection system by mammographic appearance and histopathology, " Cancer, 104(5):931-935, 2005.

[54] C. G. Berman, "Recent advances in breast-specific imaging, "Cancer control, 14(4):338-349, 2007.

[55] S. Ciatto, N. Houssami, D. Gur, R. Nishikawa, R. Schmidt, C. Metz, J. Ruiz, S. Feig, R. Birdwell, M. Linver, J. Fenton, W. Barlow, J. Elmore, "Computer-aided screening mammography," The New England Journal of Medicine (NEJM), 357(1):83-85, 2007.

[56] J. G. Fletcher, W. Luboldt, "CT colonography and MR colonography: current status, research directions and comparison," European Radiology, 10:786-801, 2000.

[57] W. Luboldt, J. G. Fletcher, T. J. Vogl, "Colonography: current status, research directions and challenges," European Radiology, 12(3):502-524, 2002.

[58] C. G. Coin, F. C. Wollett, J. T. Coin, M. Rowland, R. K. DeRamos, R. Dandrea, "Computerized radiology of the colon: A potential screening technique, " Computerized Radiology, 7(4):215-221, 1983.

[59] D. J. Vining, D. W. Gelfand, "Noninvasive colonoscopy using Helical CT scanning, 3D reconstruction, and virtual reality, "The 23rd Annual Meeting of the Society of Gastrointestinal Radiologists, 1994.

[60] D. Bielen, G. Kiss, "Computer-aided detection for CT colonography: Update 2007," Abdominal Imaging, 32(5):571-581, 2007.

[61] J. H. Yao, M. Miller, M. Franaszek, R. M. Summers, "Colonic polyp segmentation in CT colonography-based on fuzzy clustering and deformable models, "IEEE Transactions on Medical Imaging, 23(11):1344-1352, 2004.

[62] A. Jerebko, S. Lakare, P. Cathier, S. Periaswamy, L. Bogoni, "Symmetric curvature patterns for colonic polyp detection, "Proceedings of the International Conference on Medical Image Computing and Computer-Assisted Intervention (MICCAI), LNCS 9(2):169-176, 2006.

[63] Ziosoft: http://www.zio.co.jp/

[64] GE: http://www.ge.com/

[65] Siemens: http://w1.siemens.com/

[66] J. Nappi, H. Yoshida, "Feature-guided analysis for reduction of false positives in CAD of polyps for computed tomographic colonography," Medical Physics, 30(7):1592-1601, 2003

[67] D. S. Paik, C. F. Beaulieu, G. D. Rubin, B. Acar, R. B. Jeffrey, J. Yee, J. Dey, S. Napel, "Surface normal overlap: a computer-aided detection algorithm with application to colonic polyps and lung nodules in helical CT," IEEE Transaction on Medical Imaging, 23(6):661-675, 2004

[68] J. Sosna, M. M. Morrin, J. B. Kruskal, "CT colonography of colorectal polyps: a meta analysis," American Journal of Roentgenology, 181(6):1593-1598, 2003

[69] J. K. Frost, W. C. Ball, M. L. Levin, M. S. Tockman, R. R. Baker, D. Carter, J. C. Eggleston, Y. S. Erozan, P. K. Gupta, N. F. Khouri, "Early lung cancer detection: results of the initial (prevalence) radiologic and cytologic screening in the Johns Hopkins study," American Thoracic Society: Diagnostic, 130(4):549-554, 1984.

[70] B. J. Flehinger, M. R. Melamed, M. B. Zaman, R. T. Heelan, W. B. Perchick, N. Martini, "Early lung cancer detection: results of the initial (prevalence) radiologic and cytologic screening in the Memorial Sloan-Kettering study," American Thoracic Society Diagnostic, 130(4):550-560, 1984.

[71] M. L. Giger, K. Doi, H. MacMahon, "Image feature analysis and computer-aided diagnosis in digital radiography. 3. Automated detection of nodules in peripheral lung fields," Medical Physics, 15(2):158-66, 1988.

[72] X. W. Xu, K. Doi, T. Kobayashi, H. MacMahon, M. L. Giger, "Development of an improved CAD scheme for automated detection of lung nodules in digital chest images," Medical Physics, 24(9):1395-03, 1997.

[73] T. Ishida, S. Katsuragawa, K. Nakamura, K. Ashizawa, H. MacMahon, K. Doi, "Computerized analysis of interstitial lung diseases on chest radiographs based on lung texture, geometric-pattern features and artificial neural networks," Proceedings of SPIE Medical imaging, 4684:1331-8, 2002.

[74] J. Wei, Y. Hagihara, A. Shimizu, H. Kobatake, "Optimal image feature set for detecting lung nodules on chest X-ray images," Proceedings of International Workshop on Computer-Aided Diagnosis, CARS 2002:706-711, 2002.

[75] J. Shiraishi, H. Abe, R. Engelmann, M. Aoyama, H. MacMahon, K. Doi, "Computer-aided diagnosis for distinction between benign and malignant solitary pulmonary nodules in chest radiographs: ROC analysis of radiologists' performance," Radiology, 227(2):469-74, 2003.

[76] T. Okumura, T. Miwa, J. Kako, S. Yamamoto, M. Matsumoto, Y. Tateno, T. Iinuma, and T. Matsumoto, "Image processing for computer-aided diagnosis of lung cancer screening system by CT (LSCT)," Proceedings of SPIE Medical imaging, 3338:1314-1322, 1998.

[77] T. Nawa, T. Nakagawa, S. Kusano, Y. Kawasaki, Y. Sugawara, and H. Nakata, "Lung cancer screening using low-dose spiral CT: Results of baseline and 1-year follow-up studies," Chest, 122(1):15-20, 2002.

[78] S. Sone, F. Li, Z. G. Yang, T. Honda, Y. Maruyama, S. Takashima, M. Hasegawa, S. Kawakami, K. Kubo, K. M. Haniuda, "Results of three-year mass screening pro-

gramme for lung cancer using mobile low-dose spiral computed tomography scanner," British Journal of Cancer, 84(1):25-32, 2001.

[79] S. J. Swensen, J. R. Jett, T. E. Hartman, D. E. Midthun, S. J. Mandrekar, S. L. Hillman, A. M. Sykes, G. L. Aughenbaugh, and A. O. B. L. Allen, "CT screening for lung cancer: Five-year prospective experience," Radiology, 235(1):259-265, 2005.

[80] Q. Li, S. Sone, K. Doi, "Selective enhancement filters for nodules, vessels, and airway walls in two- and three-dimensional CT images," Medical Physics, 30(8):2040-2051, 2003.

[81] Y. Lee, T. Hara, H. Fujita, S. Itoh, T. Ishigaki, "Automated detection of pulmonary nodules in helical ct images based on an improved template- matching technique," IEEE Transaction on Medical Imaging, 20(7):595-604, 2001.

[82] L. Boroczky, L. Zhao, K. P. Lee, "Feature subset selection for improving the performance of false positive reduction in lung nodule CAD," Proceedings of IEEE Symposium on Computer-Based Medical Systems, 10:85-90, 2005.

[83] L. P. Lawler, S. A. Wood, H. S. Pannu, E. K. Fishman, "Computer-assisted detection of pulmonary nodules: preliminary observations using a prototype system with multi detector-row CT data sets," Journal of Digital Imaging, 16(3):251-261, 2003.

[84] K. Marten, C. Engelke, T. Seyfarth, A. Grillhosl, S. Obenauer, "Computer-aided detection of pulmonary nodules: Influence of nodule characteristics on detection performance," Clinical Radiology, 60(2):196-206, 2005.

[85] S. Armato, M. Giger, H. MacMahon, "Automated detection of lung nodules in CT images: preliminary results," Medical Physics, 28(8):1552-1561, 2001.

[86] S. Armato, M. Altman, P. J. La Riviere, "Automated detection of lung nodules in CT images: Effect of image reconstruction algorithm," Medical Physics, 30(3):461-472, 2003.

[87] B. S. Zhao, G. Gamsu, M. S. Ginsburg, L. Jiang, L. H. Schwartz, "Automatic detection of small lung nodules on CT utilizing a local density maximum algorithm," Journal of Applied Clinical Medical Physics, 4(3):248-260, 2003.

[88] M. N. Gurcan, B. Sahiner, N. Petrick, H.-P. Chan, E. A. Kazerooni, P. N. Cascade, L. Hadjiski, "Lung nodule detection on chest computed tomography images: preliminary evaluation of a computer-aided diagnosis system. " Medical Physics, 29(11):2552-2558, 2002.

[89] C. C. McCulloch, R. A. Kaucic, P. R. S. Mendonca, D. J. Walter, R. S. Avila, "Model-based detection of lung nodules in computed tomography exams," Academic Radiology, 11(3):258-266, 2004.

[90] S. Ozekes, O. Osman, "Computerized lung nodule detection using 3D feature extraction and learning based algorithms," Journal of Medical Systems, 34(2):185-194, 2008.

[91] H. Takizawa, S. Yamamoto, T. Shiina, "Recognition of pulmonary nodules in chest CT images using 3-D deformable object models of different classes," Algorithms, 10:125-144, 2010.

[92] M. Aoyama, Q. Li, S. Katsuragawa, F. Li, S. Sone, K. Doi, "Computerized scheme for determination of the likelihood measure of malignancy for pulmonary nodules on low-dose CT images," Medical Physics, 30(3):387-394, 2003.

[93] J. Rogowska, "Overview and fundamental of medical image segmentation," Handbook of Medical Image Processing and Analysis, I. Bankman (ed.), 73-90, 2008.

[94] A. Ez-Baz, J. S. Suri, "Lung imaging and Computer-Aided Diagnosis," CRC Press, 2011.

[95] M. Kass, A. Witkin, D. Terzopoulos, "Snakes: Active contour models," International Journal of Computer Vision, 321-331, 1988.

[96] T. Cootes, C. J. Taylor, D. Cooper, J. Graham, "Active shape models–Their training and application."Computer Vision and Image Understanding, 61(1):38-59, 1995.

[97] T. Cootes, G. J. Edwards, C. J. Taylor, "Active appearance models," IEEE Trans Pattern Analysis and Machine Intelligence, 23(6):681-685, 2001.

[98] J. A. Sethian, "Level set methods and fast marching methods: Evolving interfaces in computational geometry, fluid mechanics, computer vision and material science, " Cambridge University Press, UK, 1999.

[99] Y. Boykov, O. Veksler, R. Zabih, "Fast approximate energy minimisation via graph cuts," IEEE Trans Pattern Analysis and Machine Intelligence, 23(11):1222-1239, 2001.

[100] I. C. Sluimer, M. Niemeijer, B. van Ginneken, "Lung field segmentation from thin-slice CT scans in presence of severe pathology," Proceedings of SPIE Medical Imaging, 5370:1447-1455, 2004.

[101] T. Mitchell, "Machine learning," New York: WCB McGraw-Hill, 1997

[102] R. O. DUda, P. E. Hart, D. G. Stork, "Pattern classification and scene analysis," 2nd ed., New York: John Wiley& Sons.

[103] A. A. Goshtasby, "2-D and 3-D image registration for medical, remote sensing, and industrial applications," Wiley Press, 2005.

[104] J. Maintz, M. Viergever, "A survey of medical image registration," Medical Image Analysis, 2(1):1-36, 1998.

[105] J. Pluim, J. Maintz, M. Viergever, "Mutual-information-based registration of medical images: a survey," IEEE Transactions on Medical Imaging, 22(8):986-1004, 2003

[106] H. Lester, S. Arridge, "A survey of hierarchical non-linear medical image registration," Pattern Recognition, 32(1):129-149, 1999.

[107] D. Rueckert, L. I. Sonoda, C. Hayes, D. L. Hill, M. O. Leach, D. J. Hawkes, "Non-rigid registration using free-form deformations: Application to breast mr images," IEEE Transaction on Medical Imaging, 18(8):712-721, 1999.

[108] D. Mattes, D. Haynor, H. Vesselle, T. Lewellen, W. Eubank, "Pet-ct image registration in the chest using free-form deformations," IEEE Transactions on Medical Imaging, 22(1):120-128, 2003.

[109] C. Lorenz, I. Carlsen, T. Buzug, C. Fassnacht, J. Weese, "Multiscale line segmentation with automatic estimation of width, contrast and tangential direction in 2D and 3D medical images," Proceedings of First Joint Conference on Computer Vision, Virtual Reality and Robotics in Medicine and Medical Robotics and Computer-Assisted Surgery (CVRMED-MRCAS 097), Lecture Notes in Computer Science, 1205:233-242, 1997.

[110] Y. Sato, S. Nakajima, H. Atsumi, H. Koller, G. Gerig, Y. Yoshida, R. Kikinis, "3D multi-scale line filter for segmentation and visualization of curvilinear structures in medical images," Medical Image Analysis, 2(2):143-168, 1998.

[111] Y. Sato, C. Westin, A. Bhalerao, S. Nakajima, N. Shiraga, S. Tamura, "Tissue classification based on 3D local intensity structures for volume rendering," IEEE Transaction on Visualization and Computer Graphics, 6(2):160-180, 2000.

[112] M. Descoteaux, M. Audette, K. Chinzei, K. Siddiqi, "Bone enhancement filtering: Application to sinus bone segmentation and simulation of pituitary surgery," Computer Aided Surgery, 11(5):247-255, 2006.

[113] D. S. Paik, C. F. Beaulieu, G. D. Rubin, B. Acar, R. B. Jeffrey, J. Yee, J. Dey, S. Napel, "Surface normal overlap: A computer-aided detection algorithm with application to colonic polyps and lung nodules in helical CT," IEEE Transaction on Medical Imaging, 23(6):661-675, 2004.

[114] K. Murphy, B. van Ginneken, A. M. R. Schilham, B. J. de Hoop, H. A. Gietema, and M. Prokop, "A large scale evaluation of automatic pulmonary nodule detection in chest CT using local image features and k-nearest-neighbor classification," Medical Image Analysis, 13(5):757-770, 2009.

[115] K. T. Bae, J. S. Kim, Y. H. Na, K. G. Kim, J. H. Kim. "Pulmonary nodules: Automated detection on CT images with morphologic matching algorithm: Preliminary results," Radiology, 236(1):286-294, 2005.

[116] Q. Li, K. Doi, "Analysis and minimization of over training effect in rule-based classifiers for computer-aided diagnosis," Medical Physics, 33(2):320-328, 2006.

[117] A. Retico, F. Bagagli, N. Camarlinghi, C. Carpentieri, M. E. Fantacci, and I. Gori, "A voxel-based neural approach (VBNA) to identify lung nodules in the ANODE09 study," Proceedings of SPIE Medical Imaging, 7260:72601S-1～72601S-8, 2009.

[118] R. Bellotti, P. Cerello, S. Tangaro, V. Bevilacqua, M. Castellano, G. Mastronardi, F. De Carloa, S. Bagnascob, U. Bottiglid, R. Cataldoi, E. Catanzaritig, S. C. Cheranc, P. Delogue, I. De Mitrih, G. De Nunzioi, M. E. Fantaccie, F. Faucif, G. Garganoa, B. Golosiod, P. L. Indovinag, A. Lauriag, E. Lopez Torresj, R. Magrof, G. L. Masalad, R. Massafraa, P. Olivad, A. P. Martineze, M. Quartak, G. Rasof, A. Retico, M. Sittal, S. Stumbod, A. Tatae, S. Squarciao, A. Schenoneo, E. Molinario, B. Canesi "Distributed medical images analysis on a grid infrastructure," Future Generation Computer Systems, 23(3):475-484, 2007.

[119] K. Suzuki, S. Armato, F. Li, K. Doi, "Massive training artificial neural network (MTANN) for reduction of false positives in computerized detection of lung nodules in low-dose computed tomography," Medical Physics, 30(7):1602-1617, 2003.

[120] T. Messay, R. C. Hardie, S. K. Rogers, "A new computationally efficient CAD system for pulmonary nodule detection in CT imagery," Medical Image Analysis, 14(3):390-406, 2010.

[121] R. Hardie, S. Rogers, T. Wilson, A. Rogers, "Performance analysis of a new computer aided detection system for identifying lung nodules on chest radiographs," Medical Image Analysis, 12(3):240-258, 2008.

[122] P. Croisille, M. Souto, M. Cova, S. Wood, Y. Afework, J. Kuhlman, E. Zerhouni, "Pulmonary nodules: improved detection with vascular segmentation and extraction with spiral CT," Radiology, 197(2):397-401, 1995.

[123] G. Agam, S. Armato, C. H. Wu," Vessel tree reconstruction in chest CT images with application to nodule detection," IEEE Transaction on Medical Imaging, 24(4):486-499, 2005.

[124] B. van Ginneken, S. G. Armato, B. de Hoop, S. van de Vorst, T. Duindam, M. Niemeijer, K. Murphy, A. M. R. Schilham, A. Retico, M. E. Fantacci, N. Camarlinghi, F. Bagagli, I. Gori, T. Hara, H. Fujita, G. Gargano, R. Bellotti, S. S. Tangaro, L. Bolanos, F. D. Carlo, R. Megna, S. Tangaro, L. Bolanos, P. Cerello, S. C. Cheran, E. L. Torres, M. Prokop, "Comparing and combining algorithms for computer-aided detection of pulmonary nodules in computed tomography scans: The ANODE09 study," Medical Image Analysis, 14(6):707-722, 2009.

[125] P. J. Yim, P. L. Choyke, R. M. Summers, "Gray-scale skeletonization of small vessels in magnetic resonance angiography," IEEE Transaction on Medical Imaging, 19(6):568-576, 2000.

[126] H. Schmitt, M. Grass, V. Rasche, O. Schramm, S. Haehnel, K. Sartor, "An x-ray-based method for the determination of the contrast agent propagation in 3-d vessel structures," IEEE Transaction on Medical Imaging, 21(3):251-262, 2002.

[127] E. Sorantin, C. Halmai, B. Erdohelyi, K. Palagyi, L. Nyul, K. Olle, B. Geiger, F. Lindbichler, G. Friedrich, K. Kiesler, "Spiral-ct-based assessment of tracheal stenoses using 3-D skeletonization," IEEE Transaction on Medical Imaging, 21(3):263-273, 2002.

[128] D. Guo, P. Richardson, "Automatic vessel extraction from angiogram images." IEEE Computers in Cardiology, 25:441-444, 1998.

[129] S. Eiho, Y. Qian, "Detection of coronary artery tree using morphological operator," IEEE Computers in Cardiology, 24:525-528, 1997.

[130] L. Raghupathi, S. Lakare, "A hybrid lung and vessel segmentation algorithm for computer aided detection of pulmonary embolism," Proceedings of SPIE Medical Imaging, 7260(33):1-9, 2009.

[131] R. Toledo, X. Orriols, X. Binefa, P. Raveda, J. Vitria, J. J. Villanueva, "Tracking elongated structures using statistical snakes," Proceedings of the IEEE Conference on Computer Vision and Pattern Recognition, 1:157-162, 2000.

[132] L. Sarry, J. Y. Boire, "Three-dimensional tracking of coronary arteries from biplane angiographic sequences using parametrically deformable models," IEEE Transaction on Medical Imaging, 20(12):1341-1351, 2001.

[133] F. Quek, C. Kirbas, "Vessel extraction in medical images by wave propagation and traceback," IEEE Transaction on Medical Imaging, 20(2):117-131, 2001.

[134] H. M. Zhang, Z. Z. Bian, D. Z. Jiang, Z. J. Yuan, M. Ye, "Level set method for pulmonary vessels extraction," IEEE Conference on Image Processing, 3:1105-1108, 2003.

[135] R. Poli, G. Valli, "An algorithm for real-time vessel enhancement and detection." Computer Methods and Proceedings in Biomedicine, 52(1):1-22, 1997.

[136] A. F. Frangi, W. J. Niessen, K. L. Vincken, M. A. Viergever, "Multiscale vessel enhancement filtering," In Proceedings of the International Conference on Medical Image Computing and Computer-Assisted Intervention (MICCAI), 1496:130-137, 1998.

[137] M. Descoteaux, L. Collins, K. Siddiqi, "A geometric flow for segmenting vasculature in proton-density weighted MRI," Medical Image Analysis, 12(4):497-513, 2008.

[138] K. Krissian, G. Malandain, N. Ayache, "Model based detection of tubular structures in 3D images," Computer Vision and Image Understanding 80(2):130-171, 2000.

[139] H. Shikata, E.A. Hoffman, M. Sonka, "Automated segmentation of pulmonary vascular tree from 3D CT images," Proceedings of SPIE Medical Imaging, 5369:107-116, 2004.

[140] M. Feuerstein, T. Kitasaka, K. Mori, "Automated anatomical likelihood driven extraction and branching detection of aortic arch in 3-D chest CT," The Second International Workshop on Pulmonary Image Analysis, MICCAI 2009:49-60, 2009.

[141] T. Kitasaka, K. Mori, J. Hasegawa, J. Toriwaki, "Lung area extraction from 3-D chest X-ray CT images using the shape model generated by variable Bezier surface," IEICE Transaction on Information and Systems, J83-D-2(1):165-174, 2000.

[142] T. Kitasaka, K. Mori, J. Hasegawa, J. Toriwaki, "A method for extraction of bronchus regions from 3D chest X-ray CT images by analyzing structural features of bronchus," Forma, 17:321-338, 2002.

[143] T. Lindeberg, "On scale detection for differential operators," Proceedings 8th imagedinavian Conference on Image Analysis, 857-866, 1993.

[144] M. Oda, T. Kitasaka, K. Mori, Y. Suenaga, T. Takayama, H. Takabatake, M. Mori, S. Nawano, "Digital bowel cleansing free detection method of colonic polyp from fecal tagging CT images," Academic Radiology, 16(4):486-494, 2008.

[145] B. Chen, T. Kitasaka, H. Honma, H. Takabatake, M. Mori, H. Natori, K. Mori, "Pulmonary blood vessel bifurcation enhancement filter with application to re-

duce false positive of nodule detection in 3D chest CT data," Computer Assisted Radiology and Surgery (CARS) 2010, 5(1):S95-S96, 2010.

[146] D. F. Yankelevitz, A. P. Reeves, W. J. Kostis, B. Zhao, C. I. Henschke, "Small pulmonary nodules: volumetrically determined growth rates based on CT evaluation," Radiology, 217(1):251-256, 2000.

[147] E. R. Heitzman, "The role of computed tomography in the diagnosis and management of lung cancer: an overview," Chest, 89(4):237S-241S, 1986.

[148] S. Sun, G. Rubin, D. Paik, R. M. Steiner, F. Zhuge, S. Napel, "Registration of lung nodules using semi-rigid model: Method and preliminary results," Medical Physics, 34(2):265-281, 2007.

[149] F. Beyer, D. Wormanns, C. Novak, H. Shen, B. L. Odry, G. Kohl, W. Heindel, "Clinical evaluation of a software for automated localization of lung nodules at follow-up CT examinations," Rofo, 176(6):829-836, 2004.

[150] T. Cheng, S. David, Z. Fang, K. Thomas, Pilgram, H. W. Jin, T. B. Kyongtae, "Automated matching of pulmonary nodules: Evaluation in serial screening chest CT," American Journal of Roentgenology, 192(3):624-628, 2009.

[151] T. Blaffert, R. Wiemker, "Comparison of different follow-up lung registration methods with and without segmentation," Proceedings of SPIE Medical Imaging, 5370:1701-1708, 2004.

[152] T. Kusanagi, Y. Mekada, J. Hasegawa, J. Toriwaki, M. Mori, H. Natori, "Correspondence of lung nodules in sequential chest CT images for quantification of the curative effect," International Congress Series, 1256:983-989, 2003.

[153] M. Kubo, T. Yamamoto, Y. Kawata, N. Niki, K. Eguchi, H. Ohmatsu, R. Kakinuma, M. Kaneko, M. Kusumoto, N. Moriyama, K. Mori, H. Nishiyama, "CAD system for

the assistance of comparative reading for lung cancer using serial helical CT images," Proceedings of the International Conference on Medical Image Computing and Computer-Assisted Intervention (MICCAI) LNCS, 2208:1388-1390, 2001.

[154] M. Betke, H. Honga, D. Thomasa, C. Prince, J. P. Ko, "Landmark detection in the chest and registration of lung surfaces with an application to nodule registration," Medical Image Analysis, 7(3):265-281, 2003.

[155] H. Hong, J. Leeb, Y. Yim, "Automatic lung nodule matching on sequential CT images," Computers in Biology and Medicine, 38(5):623-634, 2008.

[156] A. P. Reeves, A. B. Chan, D. F. Yankelevitz, C. I, Henschke, B. Kressler, W. J. Kostis, "On measuring the change in size of pulmonary nodules," IEEE Transaction on Medical Imaging, 25(4):435-450, 2006.

[157] A. El-Baz, S. Yuksel, S. Elshazly, A. A. Faragi, "Non-rigid registration techniques for automatic follow-up of lung nodules," Computer Assisted Radiology and Surgery (CARS) 2005, 1281:1115-1120, 2005.

[158] M. Fukui, T. Kitasaka, K. Mori, Y. Suenaga, Y. Mekada, M. Mori, H. Takabatake, H. natori, "A study on a method for finding corresponding pairs of lung nodules from follow-up chest CT scans based on non-rigid image registration," IEICE technical report, MI105(580):125-128, 2006.

[159] W. Mullally, M. Betke, H. Hong, J. Wang, K. Mann, J. P. Ko, "Multicriterion 3D segmentation and registration of pulmonary nodules on CT: A preliminary investigation," Proceedings of the International Conference on Diagnostic Imaging and Analysis (ICDIA), 176-181, 2002.

[160] B. Chen, H. Naito, Y. Nakamura, T. Kitasaka, D. Rueckert, H. Honma, H. Takabatake, M. Mori, H. Natori, K. Mori, "Automatic segmentation and identification of solitary pulmonary nodules on follow-up CT scans based on local intensity

structure analysis and non-rigid image registration," Proceedings of SPIE Medical Imaging, 7963:49-60, 2011.

[161] M. Feuerstein, T. Kitasaka, K. Mori, "Automated anatomical likelihood driven extraction and branching detection of aortic arch in 3-D chest CT," The 2nd International Workshop on Pulmonary Image Analysis, MICCAI, LNCS 1268:49-60, 2009.

[162] http://www.mrf-registration.net/

[163] C. Henschke, D. Yankelevitz, R. Mirtcheva, "CT screening for lung cancer: frequency and significance of part-solid and nonsolid nodules," American Journal of Roentgenology, 178(5):1053-1057, 2002.

[164] K. Mori, J. Hasegawa, Y. Suenaga, and J. Toriwaki. "Automated anatomical labeling of the bronchial branch and its application to the virtual bronchoscopy system," IEEE Transaction on Medical Imaging, 19(2):103-114, 2000.

[165] K. Mori, D. Deguchi, K. Akiyama, T. Kitasaka, C. R. Maurer Jr., Y. Suenaga, H. Takabatake, M. Mori, and H. Natori. "Hybrid bronchoscope tracking using a magnetic tracking sensor and image registration," Proceedings of the International Conference on Medical Image Computing and Computer-Assisted Intervention (MICCAI), LNCS 3750:543-550, 2005.

[166] D. Deguchi, K. Mori, M. Feuerstein, T. Kitasaka, C. R. Maurer Jr., Y. Suenaga, H. Takabatake, M. Mori, and H. Natori. "Selective image similarity measure for bronchoscope tracking based on image registration," Medical Image Analysis, 13(4):621-633, 2009.

[167] X. B Luo, M. Feuerstein, D. Deguchi, T. Kitasaka, H. Takabatake, K. Mori. "Development and comparison of new hybrid motion tracking for bronchoscopic navigation," Medical Image Analysis, DOI: 10.1016j.media.2010.11.001. 2010.

[168] X. B. Luo, T. Kitasaka, K. Mori, "ManiSMC: a new method using manifold modeling and sequential Monte Carlo sampler for boosting navigated bronchoscopy," Proceedings of the International Conference on Medical Image Computing and Computer-Assisted Intervention (MICCAI), LNCS 6893:248-255, 2011.

Publications

Journal papers

(1) **B. Chen**, Y. Nakamura, T. Kitasaka, H. Honma, H. Takabatake, M. Mori, H. Natori, K. Mori, "Method for Matching Small Pulmonary Nodules That Is Robust to Temporal Changes on Follow-up Thoracic CT Images (in Japanese)," Medical Imaging Technology, 29(4):191-199, 2011.

(2) **B. Chen**, T. Kitasaka, H. Honma, H. Takabatake, M. Mori, H. Natori, K. Mori, "Segmentation of Pulmonary Blood Vessel and Nodule Based on Local Intensity Structure Analysis and Surface Propagation in 3D Thoracic CT images," International Journal of Computer Assisted Radiology and Surgery, Doi. 10.1007/s11548-011-0638-5, 2011.

Conference papers (International)

(1) **B. Chen**, T. Kitasaka, H. Honma, H. Takabatake, M. Mori, H. Natori, K. Mori, "Automatic segmentation of solitary pulmonary nodules based on local intensity structure analysis and 3D neighborhood features in 3D chest CT images," Proceedings of SPIE Medical Imaging, 8315-116, 2012.

(2) **B. Chen**, T. Kitasaka, H. Honma, H. Takabatake, M. Mori, H. Natori, K. Mori, "Segmentation of lung metastasis on thoracic CT images based on local intensity structure analysis and pulmonary blood vessel information," Proceedings of Computer Assisted Radiology and Surgery (CARS 2011), 6(1):S371-S372, 2011.

(3) **B. Chen**, H. Naito, Y. Nakamura, T. Kitasaka, H. Honma, H. Takabatake, M. Mori, H. Natori, K. Mori, "A CAD system for automatic detection and identification of solitary pulmonary nodules on follow-up CT scans based on local intensity structure analysis and non-rigid image registration," Proceedings of SPIE Medical Imaging, 7963-10, 2011.

(4) **B. Chen**, T. Kitasaka, H. Honma, H. Takabatake, M. Mori, H. Natori, K. Mori, "Pulmonary blood vessel bifurcation enhancement filter with application to reduce false positive of nodule detection in 3D chest CT data," Proceedings of Computer Assisted Radiology and Surgery (CARS 2010), 5(1):S95-S96, 2010.

(5) **B. Chen**, H. Naito, T. Kitasaka, H. Honma, H. Takabatake, M. Mori, H. Natori, K. Mori, "Pulmonary vessel area extraction with application to reduce false positive of nodule detection in 3D chest CT data," International Forum on Medical Imaging in Asia (IFMIA), IEICE Technique Report, MI108(385):305-310, 2009.

Conference papers (Japanese)

(1) **B. Chen**, T. Kitasaka, H. Honma, H. Takabatake, M. Mori, H. Natori, K. Mori, "A study on automatic detection of lung nodule based on local intensity structure analysis and 3D neighborhood features in 3-D chest CT images (in Japanese)," Proceedings of Japan Society of Computer Aided Surgery (JSCAS 2011), 13(3):356-357, 2011

(2) M. Kishi, **B. Chen**, M. Oda, T. Kitasaka, S. Iwano, K. Mori, "Automated extraction of lymph nodes from chest contrast enhanced CT images using local intensity structure analysis to assist decision puncture position for bronchoscopy (in Japanese)," Proceedings of Japan Society of Computer Aided Surgery (JSCAS2011), 13(3)::358-359, 2011.

(3) M. Minatsu, **B. Chen**, X. B. Luo, M. Oda, T. Kitasaka, H. Honma, H. Takabatake, M. Mori, H. Natori, K. Mori, "Study on improvement endoscope position iden-

tification for bronchoscope navigation based on eigenspace image matching (in Japanese)," Proceedings of Japan Society of Computer Aided Surgery (JSCAS 2011), 13(3):268-269, 2011.

(4) **B. Chen**, Y. Nakamura, T. Kitasaka, H. Honma, H. Takabatake, M. Mori, H. Natori, K. Mori, "A method for matching of small pulmonary nodules with robust to the temporal change from follow-up thoracic CT scans (in Japanese)," Proceedings of Japanese Society of Medical Imaging Technology (JAMIT 2011), OP5-3, 2011.

(5) M. Minatsu, **B. Chen**, X. B. Luo, M. Oda, T. Kitasaka, H. Honma, H. Takabatake, M. Mori, H. Natori, K. Mori, "Endoscope position identification for bronchoscope navigation based on eigenspace image matching (in Japanese)," Proceedings of Japanese Society of Medical Imaging Technology (JAMIT 2011), OP8-4, 2011.

(6) M. Kishi, **B. Chen**, T. Kitasaka, S. Iwano, K. Mori, "Automated extraction of lymph nodes from 3D chest CT images using local intensity structure analysis (in Japanese)," Proceedings of Japanese Society of Medical Imaging Technology (JAMIT 2011), OP5-9, 2011.

(7) **B. Chen**, Y. Nakamura, T. Kitasaka, H. Honma, H. Takabatake, M. Mori, H. Natori, K. Mori, "Automatic identification of small pulmonary nodules on follow-up CT scans based on non-rigid image registration (in Japanese)," Proceedings of Japan Society of Computer Aided Surgery (JSCAS 2010), 12(3):450-451, 2010.

(8) **B. Chen**, T. Kitasaka, H. Honma, H. Takabatake, M. Mori, H. Natori, K. Mori, "A study on construction of simultaneous recognition system of pulmonary blood vessels and nodules from chest X-ray CT image (in Japanese)," Proceedings of Japanese Society of Medical Imaging Technology (JAMIT 2010), OP6-5, 2010.

(9) **B. Chen**, T. Kitasaka, H. Honma, H. Takabatake, M. Mori, H. Natori, K. Mori, "A study on extraction of pulmonary vascular with discrimination of nodules from chest CT image (in Japanese)," Proceedings of Japan Society of Computer Aided Surgery (JSCAS 2009), 11(3):404-405, 2009.

(10) H. Naito, **B. Chen**, K. Mori, Y. Suenaga, T. Kitasaka, H. Honma, H. Takabatake, M. Mori, H. Natori, "Methods for identifying small pulmonary nodules on follow-up CT scans using non-rigid registration (in Japanese)," IEICE Technique Report, PRMU2008-287:313-318, 2009.

(11) Y. Nakamura, **B. Chen**, T. Kitasaka, H. Honma, H. Takabatake, M. Mori, H. Natori, K. Mori, " Method for identifying multiple small pulmonary nodules on follow-up CT scans using non-rigid registration (in Japanese)，"Proceedings of Tokai-Section Joint Conference on Electrical and Related Engineering (TJCERE 2009), O-116, 2009.

(12) **B. Chen**, Y. Nakamura, T. Kitasaka, K. Mori, Y. Suenaga, H. Honma, H. Takabatake, M. Mori, H. Natori, "A study on extraction of pulmonary vascular from chest CT image based on Level-set method using local intensity structures analysis (in Japanese)," Proceedings of Japanese Society of Medical Imaging Technology (JAMIT 2009), OP1-08, 2009.

(13) **B. Chen**, M. Oda, T. Kitasaka, K. Mori, Y. Suenaga, H. Honma, H. Takabatake, M. Mori, H. Natori, "A study on automated extraction of pulmonary vessels from 3D chest CT data using Level-set method (in Japanese)," Proceedings of Japanese Society of Medical Imaging Technology (JAMIT 2008)，C1-01，2008.

(14) **B. Chen**, Y. Nakamura, K. Mori, Y. Suenaga, T. Kitasaka, H. Honma, H. Takabatake, M. Mori, H. Natori, "A study on automated extraction of pulmonary vessels from 3D Chest CT images based on Level-set method (in Japanese)，"Proceedings of Tokai-Section Joint Conference on Electrical and Related Engineering (TJCERE 2008)，O-490，2008.